Coupling a Markov Chain and Support Vector Machine for At-Site Downscaling of Daily Precipitation

YU-KUN HOU AND HUA CHEN

State Key Laboratory of Water Resources and Hydropower Engineering Science, Wuhan University, Wuhan, China

CHONG-YU XU

State Key Laboratory of Water Resources and Hydropower Engineering Science, Wuhan University, Wuhan, China, and Department of Geosciences, University of Oslo, Oslo, Norway

JIE CHEN AND SHENG-LIAN GUO

State Key Laboratory of Water Resources and Hydropower Engineering Science, Wuhan University, Wuhan, China

(Manuscript received 7 June 2016, in final form 27 June 2017)

ABSTRACT

Statistical downscaling is useful for managing scale and resolution problems in outputs from global climate models (GCMs) for climate change impact studies. To improve downscaling of precipitation occurrence, this study proposes a revised regression-based statistical downscaling method that couples a support vector classifier (SVC) and first-order two-state Markov chain to generate the occurrence and a support vector regression (SVR) to simulate the amount. The proposed method is compared to the Statistical Downscaling Model (SDSM) for reproducing the temporal and quantitative distribution of observed precipitation using 10 meteorological indicators. Two types of calibration and validation methods were compared. The first method used sequential split sampling of calibration and validation periods, while the second used odd years for calibration and even years for validation. The proposed coupled approach outperformed the other methods in downscaling daily precipitation in all study periods using both calibration methods. Using odd years for calibration and even years for validation can reduce the influence of possible climate change–induced nonstationary data series. The study shows that it is necessary to combine different types of precipitation state classifiers with a method of regression or distribution to improve the performance of traditional statistical downscaling. These methods were applied to simulate future precipitation change from 2031 to 2100 with the CMIP5 climate variables. The results indicated increasing tendencies in both mean and maximum future precipitation predicted using all the downscaling methods evaluated. However, the proposed method is an at-site statistical downscaling method, and therefore this method will need to be modified for extension into a multisite domain.

1. Introduction

Increasing concentrations of greenhouse gases in the atmosphere have accelerated global and regional climate change; as a result, global climatic change has become a globally popular research topic (Boé et al. 2007; Chen et al. 2011; Pavlik et al. 2014; Marhaento et al. 2016; Li et al. 2016; Awan et al. 2016). Global climate models (GCMs), originally aimed at predicting area-average, synoptic-scale, and general circulation patterns of the atmosphere, have been used extensively to provide potential climatic change scenarios (Xu 1999; Xu et al. 2005). However, the coarse resolution of GCMs results in an imprecise explanation of regional precipitation, which is a stochastic variable that occurs at finer spatial-scale geographic grids than those of GCMs. Therefore, downscaling techniques have been proposed to relate large-scale atmospheric variables to local- or station-scale meteorological variables and manage the differences in the spatial scale to improve the accuracy of GCM outputs at smaller scales (Rudd and Kay 2016).

Downscaling techniques are generally divided into two categories: dynamical downscaling (DD) and statistical downscaling (SD). Dynamical downscaling achieves a

Corresponding author: Hua Chen, chua@whu.edu.cn

DOI: 10.1175/JHM-D-16-0130.1

higher spatial resolution of atmospheric physics in a limited area by combining regional climate models (RCMs) with corresponding boundary conditions from GCMs (Giorgi et al. 2001; Xu et al. 2005). RCMs provide more detailed precipitation dynamics than GCMs. Recent studies have focused on RCM ensemble forecasting (e.g., Rockel and Woth 2007; Nowreen et al. 2015). However, RCMs require considerable computing resources and are as expensive to run as a global GCM; therefore, the availability of higher-resolution long-term data remains limited (Plummer et al. 2006; J. Chen et al. 2012b). Many applications still need to downscale the results from such models to individual sites or localities for impact studies (J. Chen et al. 2014a). Statistical downscaling has been widely applied to climate change studies because of its simplicity and flexibility (Wilby et al. 1998; Zorita and Von Storch 1999; Diaz-Nieto and Wilby 2005; Liu et al. 2012). Statistical downscaling links the spatial-scale GCM or RCM output variables (predictors) to the local- or station-scale observed variables (predictands) by employing mathematical and statistical methods. Compared with dynamical downscaling, statistical downscaling requires fewer calculations and is easier for users to apply (Ghosh and Mujumdar 2008; Jacobeit et al. 2014).

According to Maraun et al. (2010), statistical downscaling can be classified into three main types: perfect prognosis (PP; Bürger and Chen 2005; Mandal et al. 2016), stochastic weather generators (WGs; Wilby and Wigley 1997; Chen et al. 2017), and model output statistics (MOS; Rummukainen 1997; Chen et al. 2016). PP downscaling methods construct a relationship between meteorological predictors and observed predictands, including weather typing and regression-based downscaling approaches. One representative method for weather typing is the analog method, which generates climate series and meteorological parameters from resampling local observed data with anomalies among the simulations from different time periods (Zorita and Von Storch 1999; Hewitson and Crane 2002; Wetterhall et al. 2005; Paredes et al. 2006; Cheng et al. 2010; Osca et al. 2013).

Regression-based downscaling methods are designed to construct an empirical statistical relationship between large-scale predictors and local-scale predictands with a regression algorithm. Regression-based downscaling methods offer good performance in simulating precipitation amounts, especially on long time scales (Dibike and Coulibaly 2005; Liu et al. 2012). Multiple studies have focused on the dimensionality reduction of input data and improvement in the regression algorithm. For example, Schubert and Henderson-Sellers (1997) integrated all available variables of a GCM into six principal components as the input of a multiple linear regression (MLR) to improve temperature downscaling in Australia. Crane and Hewitson (1998) used artificial neural networks (ANNs) in an empirical downscaling procedure to derive daily subgrid-scale precipitation from GCM data and succeeded in simulating the precipitation magnitude, but the ANNs frequently underestimated precipitation occurrence because ANNs generate more trace precipitation than zero data. Schoof and Pryor (2001) compared linear regression models and ANNs with the input data handled with principal components analysis (PCA) and cluster frequencies. Their results showed that the ANN was superior to the MLR and that its performance in downscaling monthly precipitation was far superior to its downscaling of daily precipitation. They also found that temperature models performed better than precipitation models because of the precipitation models' failure to represent precipitation variability on short synoptic time scales. H. Chen et al. (2010) compared a statistical downscaling approach based on the smooth support vector machine (SSVM) method with ANNs to predict the daily precipitation of changing climate in the Hanjiang River basin. The SSVM provided more satisfactory performances than ANNs in reproducing the mean value of the seasonal precipitation amount. However, the extreme daily precipitation amounts and standard deviation of daily precipitation were still poorly preserved in the SSVM. From these prior studies, it is clear that it is more effective to apply an advanced nonlinear regression algorithm in downscaling instead of MLR to simulate the magnitude of precipitation. However, because of lack of information on precipitation state classification, the disadvantage of this kind of approach is its poor performance in describing precipitation variance on daily and shorter time scales (Liu et al. 2012).

WGs are also popular downscaling methods, and much effort has been expended on downscaling WG parameters (Zhang 2005; Kilsby et al. 2007; Chen and Brissette 2014). WGs are generally two-step multivariate models: the simulation of occurrence and the calculation of amounts (Kilsby et al. 2007). The adjustment of WG parameters can be classified into two categories. The first calibrates the parameters on a daily scale using the atmospheric variables as inputs (Wilby et al. 2002a), and the second, most-used, method adjusts WG parameters based on climate change signals projected from climate models. Several WGs, such as Climate Generator (CLIGEN; Nicks et al. 1995), Long Ashton Research Station Weather Generator (LARS-WG; Semenov and Barrow 1997), Weather Generator (WGEN; Wilks 1999a), and Weather Generator of the

École de Technologie Supérieure (WeaGETS; J. Chen et al. 2012a), have been developed and used as downscaling tools for climate change impact studies. The advantage of using WGs is their ability to produce an ensemble of climate scenarios to study the impacts of risk-based climate events.

In some cases, the merits of PPs and WGs have been combined, as in the Statistical Downscaling Model (SDSM; Wilby et al. 2002b) and Automated Statistical Downscaling (ASD; Hessami et al. 2008), two of the most widely used statistical downscaling methods. They both try to combine the advantages of the regression-based downscaling technique and weather generators. For example, SDSM has two separate downscaling modules: unconditional and conditional (Wilby and Dawson 2013). The unconditional module represents a simple regression-based downscaling method with a multiple linear regression. It is suitable for series with continuous distributions, such as temperature. Meanwhile, the conditional module has an occurrence classifier to evaluate the state of the features; therefore, it is suitable for precipitation downscaling. SDSM has proven to have a good performance in downscaling climate series in different river basins (Chu et al. 2010; Tatsumi et al. 2014) and offers a better performance than the simple regression-based downscaling methods or weather generators in many cases (Khan et al. 2006; Hassan et al. 2014).

To evaluate downscaling performance, the occurrence and magnitude of precipitation need to be evaluated. In terms of the occurrence, H. Chen et al. (2012) concluded that SDSM was better than the SSVM in downscaling precipitation using statistics describing temporal and spatial characteristics. J. Chen et al. (2012b) pointed out that SDSM had a slight error in precipitation occurrence, which may have been caused by its occurrence generator, while occurrence can be well replicated with WGs. However, compared with MLR, the nonlinear regression algorithm performs better in simulating the magnitude of precipitation, and especially in reproducing extreme events (Schoof and Pryor 2001; H. Chen et al. 2010). J. Chen et al. (2014b) combined discriminant analysis and linear regression to downscale daily precipitation with different scenarios. The results showed a disappointing performance in both occurrence and magnitude.

Accordingly, based on a combination of precipitation occurrence and magnitude generator, a new approach is proposed in this study. The method integrates a common precipitation occurrence generator from WGs and a machine learning algorithm as a precipitation occurrence classifier and uses an advanced nonlinear regression algorithm as a precipitation amount generator. This approach has been applied in the Xiangjiang River basin using the following steps 1) construction and evaluation of the statistical downscaling methods by combining Markov chain (MC) and support vector machine (SVM) approaches, 2) evaluation of the uncertainty in simulating future climate change with two different climate scenarios and three different downscaling methods, and 3) evaluating different combinations of occurrence generators and precipitation generators to determine the optimal choice.

2. Method and evaluation

a. The basic algorithm for downscaling methods

A revised regression-based statistical downscaling method based on the least squares support vector machine (LS-SVM) and MC is proposed to improve simulations of precipitation magnitude and occurrence. For completeness, the procedure is described below.

1) LS-SVM

The SVM method was proposed in Vapnik (1998), based on the Vapnik–Chervonenkis (VC) dimension and structural risk minimization (SRM) of statistical learning theory. SVM is an original, small-sample learning method with a solid theoretical basis. In contrast to other statistical methods, it does not incorporate probability measures or the law of large numbers. It has been proven that the global optimal solution can theoretically be found with the SVM method. Thus, it overcomes the problem of local extremum often found in the ANN computational process. In sum, the SVM approach avoids the traditional process from induction to deduction, achieves effective transductive inference from training samples to forecast samples, and simplifies general classification and regression problems. Based on a relatively strict statistical learning theory, models established with the SVM method are capable of good generalization. The SVM can produce a strict boundary for the generalization abilities of established models, an advantage not found in other learning methods. The SVM method offers superior results in classification and regression with small samples, nonlinear relationships, and high-dimensional datasets.

However, the constrained optimization programming in SVM leads to a relatively high computation demand. The LS-SVM proposed in Suykens and Vandewalle (1999) takes the equality constraint instead of the inequality constraint in SVM to solve the problem of convex quadratic optimization. Compared with the standard SVM, LS-SVM only requires shape parameters of the kernel function and penalty coefficient, instead of the

value of the insensitive loss function (Suykens et al. 2002). It simplifies the calculation, requires less memory, and makes the algorithm practical to use, all of which makes LS-SVM more suitable for statistical downscaling than SVM. In this study, two LS-SVM modules are used: one for classification [support vector classification (SVC)] and one for regression [support vector regression (SVR)].

The first application of the LS-SVM in downscaling was to simulate monthly precipitation (Tripathi et al. 2006); since then, LS-SVM has proven to be a reliable method for conducting climate impact studies. Anandhi et al. (2008) used LS-SVM to downscale monthly precipitation to the river basin scale in India and found that the LS-SVM model was a feasible choice for obtaining future precipitation projections at a river basin scale, but that it was unable to mimic observed extreme precipitation events. More recently, LS-SVM has been widely used in regression-based downscaling methods (Raje and Mujumdar 2011; Sachindra et al. 2013).

LS-SVM assumes that there is a training set $\{\mathbf{X}_i, \mathbf{Y}_i\}_{i=1}^{l}$, where $\mathbf{X}$ represents a multidimensional input vector and $\mathbf{Y}$ is an output vector (Wang and Hu 2005). A function $\phi(\mathbf{X})$ is utilized to translate $\mathbf{X}$ from the original space into high-dimension space:

$$\phi(\mathbf{X}) = [\phi(\mathbf{X}_1), \phi(\mathbf{X}_2), \ldots, \phi(\mathbf{X}_l)]. \tag{1}$$

In the high-dimension space, an optimal decision function is constructed:

$$y = W^{\mathrm{T}}\phi(\mathbf{X}) + b, \tag{2}$$

where W and b are the parameters.

To minimize the structural risk, an objective function R is constructed as

$$R = \min\left\{\frac{1}{2}\|W\|^2 + C\sum_{i=1}^{l}\xi_i^2\right\}, \tag{3}$$

where ξ is the loss function and C is the regularization parameter, subjected to

$$y_i = W^{\mathrm{T}}\phi(\mathbf{X}_i) + b + \xi_i \quad (\zeta_i \geq 0), \quad (i = 1, \ldots, l). \tag{4}$$

This optimization problem can be solved with Lagrange multipliers:

$$L(W, b, \zeta_i, \alpha) = \frac{1}{2}\|W\|^2 + C\sum_{i=1}^{l}\xi_i^2 - \sum_{i=1}^{l}\alpha_i[W^{\mathrm{T}}\phi(\mathbf{X}_i) + \zeta_i - y_i], \tag{5}$$

where α_i is the ith Lagrange multiplier.

Setting the partial derivative of these four parameters to 0 in Eq. (5) gives

$$\frac{\partial L}{\partial W} = \frac{\partial L}{\partial b} = \frac{\partial L}{\partial \zeta_i} = \frac{\partial L}{\partial \alpha} = 0, \tag{6}$$

$$W = \sum_{i=1}^{l}\alpha_i\phi(\mathbf{X}_i), \tag{7a}$$

$$\sum_{i=1}^{l}\alpha_i = 0, \tag{7b}$$

$$\alpha_i = C\zeta_i \quad (i = 1, \ldots, l), \quad \text{and} \tag{7c}$$

$$y_i = W^{\mathrm{T}}\phi(\mathbf{X}_i) + b + \xi_i. \tag{7d}$$

A kernel function $K(\mathbf{X}_i, \mathbf{X}_j)$ that meets the Mercer condition F is one way to handle an input vector, such that

$$K(\mathbf{X}_i, \mathbf{X}_j) = F[\phi(\mathbf{X}_j), \phi(\mathbf{X}_i)]. \tag{8}$$

In LS-SVM, we generally use the radial basis function (RBF) as the kernel function:

$$K(\mathbf{X}_i, \mathbf{X}_j) = \exp[-(\mathbf{X}_i, \mathbf{X}_j)^2/2\sigma^2], \tag{9}$$

where σ is the width of a kernel, which is a positive real constant.

Finally, the determined decision function $f(\mathbf{X}_i)$ can be written as

$$f(\mathbf{X}_i) = \sum_{i=1}^{l}\alpha_i K(\mathbf{X}_i, \mathbf{X}_j) + b. \tag{10}$$

This decision function can also be regarded as a regression function instead of a classifier, which means that the LS-SVM is capable of performing high-dimensional nonlinear regressions. For the remainder of this paper, LS-SVM is shortened to SVM for convenience.

2) The generating occurrence algorithm: Markov chain

A Markov chain is selected in the proposed approach to add a stochastic term to the SVC classifier for generating precipitation and nonprecipitation occurrences, that is, a wet day or dry day. MC has proven relatively stable (Katz 1981) and is widely used in weather generators (Gregory et al. 1993; Wilks 1999b; Breinl et al. 2015). The probability of a given day being wet or dry is determined from the precipitation state of the day before.

b. Three proposed downscaling methods based on SVM: R-LD, CR-LD, and MC-LD

1) R-LD (SVR downscaling)

R-LD is a single-step downscaling method in which the large-scale climatic predictors and site-specific

observed precipitation are directly related with the SVM regression algorithm. Many researchers use this simple SVM regression method to statistically downscale the regional and at-site temperature and precipitation at daily and monthly scales (Tripathi et al. 2006; H. Chen et al. 2010; Ghosh 2010; Aksornsingchai and Srinilta 2011; Srinivas et al. 2014):

$$R_t^{\text{obs}} = F_{\text{SVR}}(u_t^1, u_t^2, \ldots, u_t^j), \tag{11}$$

where R_t^{obs} is the observed precipitation amount on day t, u_t^j is the jth corresponding climatic predictor on the tth day in the calibration period, and F_{SVR} is the constructed regression function.

This regression relationship constructed as described is then used to generate the precipitation in the validation period.

$$R_t^{\text{sim}} = F_{\text{SVR}}(\widehat{u_t^1}, \widehat{u_t^2}, \ldots, \widehat{u_t^j}), \tag{12}$$

where R_t^{sim} is the derived precipitation on the tth day and $\widehat{u_t^j}$ is the jth corresponding climatic predictor on the tth day in the validation period.

2) CR-LD (SVC-SVR DOWNSCALING)

The above-described R-LD method has a limitation: it cannot distinguish the state of precipitation. All precipitation data for both wet and dry days are used to construct the regression relationship, which makes the simulations contain more trace daily precipitation, which leads to far more wet days (values greater than 0) than observed.

Based on R-LD, the CR-LD method adds an occurrence classifier using an SVC before simulating the precipitation magnitude, as shown on the left side of Fig. 1. This CR-LD method has also been described in S. T. Chen et al. (2010). In this method, the total series of precipitation in a calibration period is divided into two categories: wet days (defined as 1) and dry days (defined as 0) after determining that the daily precipitation magnitude is larger than a given threshold (in this study, the threshold is 0.1 mm). The precipitation state and predictors are then used to construct a relationship using an SVC:

$$w_t^{\text{obs}} = F_{\text{SVC}}(u_t^1, u_t^2, \ldots, u_t^j), \tag{13}$$

where w_t^{obs} is the observed precipitation state on the tth day and F_{SVC} is the constructed occurrence classifier.

Meanwhile, the observed precipitation and corresponding predictors of wet days are utilized to generate the relationship using the SVM regression:

$$R_t^{\text{obs}} = F_{\text{SVR}}(u_t^1, u_t^2, \ldots, u_t^j) \quad w_t^{\text{obs}} = 1\,. \tag{14}$$

In the validation period, the precipitation states are first simulated, and then rainfall occurring on wet days is generated. The precipitation on dry days is set to 0:

$$W_t^{\text{SVC,vali}} = F_{\text{SVC}}(\widehat{u_t^1}, \widehat{u_t^2}, \ldots, \widehat{u_t^j}), \tag{15}$$

$$\begin{cases} R_t^{\text{sim}} = F_{\text{SVR}}(\widehat{u_t^1}, \widehat{u_t^2}, \ldots, \widehat{u_t^j}) + e & W_t^{\text{SVC,vali}} = 1 \\ R_t^{\text{sim}} = 0 & W_t^{\text{SVC,vali}} = 0 \end{cases}, \tag{16}$$

where $W_t^{\text{SVC,vali}}$ is the SVC-simulated precipitation state on the tth day in the validation period and e is a residual term, which obeys the normal distribution with zero mean and constant variance to better fit the variance in the observed series.

3) MC-CR-LD (MC-SVC-SVR DOWNSCALING)

The CR-LD downscaling method incorporates the classification of precipitation states and simulates the precipitation magnitude on wet days. In the CR-LD downscaling method, the SVC generates deterministic precipitation states based on the deterministic relationship between atmospheric variables and observed precipitation states, which cannot represent the stochastic characteristics of precipitation. However, it is necessary to add a stochastic term to the deterministic occurrence generator, a process that has proven effective in many mature statistical downscaling methods. For example, the occurrence generator of ASD and SDSM in a conditional downscaling module is based on the linear regression of predictor variables and a comparison of the regressed result to a random number (Wilby et al. 2002b; Hessami et al. 2008). Meanwhile, simple weather generators combine the random number and Markov chain to derive the stochastic occurrence series (Wilks 1999a).

Compared with these methods, the CR-LD downscaling method does not well describe the transition process for daily precipitation occurrence using randomness. Therefore, it is necessary to adjust the precipitation classifier by introducing the concept of randomness to the precipitation process.

The randomness of precipitation is mainly reflected in the difference between wet and dry days and the transition process. The MC can thus be used as an additional effective tool to generate a random occurrence to describe the transition characteristics of precipitation states. There is a difference between observed and SVC-simulated transition parameters in the calibration period, which is considered a bias between simulation and observation. Therefore, we can construct a correction parameter factor between the

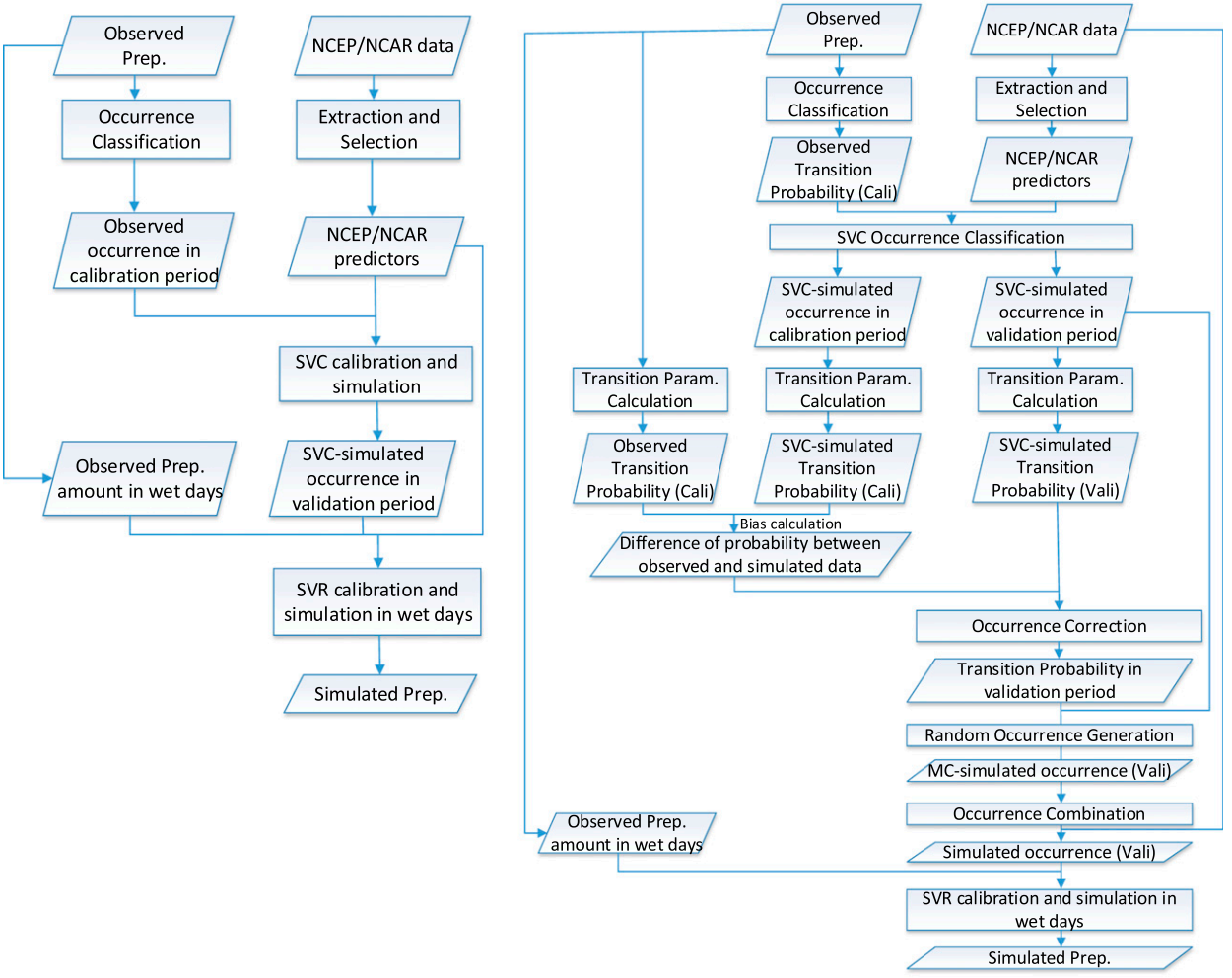

FIG. 1. (left) The CR-LD (SVC-SVR downscaling) flowchart. (right) The MC-CR-LD (MC-SVC-SVR downscaling) flowchart.

observed and SVC-simulated MC parameters in the calibration period to carry forward and then apply the bias in the MC parameters to correct SVC-simulated precipitation occurrence in the validation period. After correcting the parameters in the validation period, the generated occurrence conforms to the deterministic precipitation occurrence downscaled using the SVC of precipitation and maintains the characteristic of randomness in the validation period. The MC-CR-LD flowchart is shown on the right side of Fig. 1. In the remainder of the text, tables, and figures, we use "MC-LD" instead of "MC-CR-LD" for brevity. The modeling procedure is as follows. The precipitation state of the observed precipitation series is distinguished using a given threshold. A first-order, two-state Markov chain is utilized to distinguish the precipitation states of dry or wet days using the transition parameters. The transition probabilities of observed precipitation occurrence in the calibration period are generated by

$$\begin{aligned} P_{01}^{\text{obs,cali}} &= P\{w_t^{\text{obs}} = 1 | w_{t-1}^{\text{obs}} = 0\} \\ P_{11}^{\text{obs,cali}} &= P\{w_t^{\text{obs}} = 1 | w_{t-1}^{\text{obs}} = 1\} \end{aligned}, \tag{17}$$

where $P_{01}^{\text{obs,cali}}$ is the probability that day $t-1$ is dry and that day t is wet, as generated from the observed precipitation in the calibration period, and $P_{11}^{\text{obs,cali}}$ is the probability that the day $t-1$ is wet and day t is wet, generated from observed precipitation in the calibration period.

The bias between observed and simulated transition probabilities in the calibration period is calculated to correct probabilities in the validation period. To derive the simulated transition probabilities in the calibration period, the modeled occurrence series needs to be reproduced using the proposed downscaling model.

The SVC relationship in the calibration period is constructed using the observed occurrence and climatic predictors, which are the same as described for Eq. (13). Then, this constructed relationship F_{SVC} is utilized to simulate the precipitation state $W_t^{\mathrm{SVC,cali}}$ with the same predictors $u_t^1, u_t^2, \ldots, u_t^j$ in the calibration period.

The precipitation state transition parameters in the calibration period are derived from the SVC-simulated occurrence using the Markov chain:

$$\begin{aligned} P_{01}^{\mathrm{SVC,cali}} &= P\{W_t^{\mathrm{SVC,cali}} = 1 | W_{t-1}^{\mathrm{SVC,cali}} = 0\} \\ P_{11}^{\mathrm{SVC,cali}} &= P\{W_t^{\mathrm{SVC,cali}} = 1 | W_{t-1}^{\mathrm{SVC,cali}} = 1\} \end{aligned}. \quad (18)$$

Referencing the bias correction method (Chen et al. 2013), the bias in the state transition parameters between the observed and SVC-simulated occurrences in the calibration period is then used to adjust the SVC-simulated parameters in the validation period. The biases are quantified into two correction factors σ and γ, which are calculated below:

$$\sigma = \frac{P_{01}^{\mathrm{obs.cali}}}{P_{01}^{\mathrm{SVC,cali}}} \quad \text{and} \quad (19)$$

$$\gamma = \frac{P_{11}^{\mathrm{obs.cali}}}{P_{11}^{\mathrm{SVC,cali}}}. \quad (20)$$

Meanwhile, the SVC-simulated occurrence in the validation period is calculated by

$$W_t^{\mathrm{SVC,vali}} = F_{\mathrm{SVC}}(\widehat{u_t^1}, \widehat{u_t^2}, \ldots, \widehat{u_t^j}), \quad (21)$$

where $W_t^{\mathrm{SVC,vali}}$ is the SVC-simulated precipitation state on the tth day in the validation period and $\widehat{u_t^j}$ is the jth corresponding climatic predictor on the tth day in the validation period.

Then, the SVC-simulated transition parameters $P_{01}^{\mathrm{SVC,cali}}$ and $P_{11}^{\mathrm{SVC,cali}}$ in the validation period are calculated using $W^{\mathrm{SVC,vali}}$ and the correction factors:

$$\begin{aligned} P_{01}^{\mathrm{SVC,vali}} &= P\{W_t^{\mathrm{SVC,vali}} = 1 | W_{t-1}^{\mathrm{SVC,vali}} = 0\} \\ P_{11}^{\mathrm{SVC,vali}} &= P\{W_t^{\mathrm{SVC,vali}} = 1 | W_{t-1}^{\mathrm{SVC,vali}} = 1\} \end{aligned}. \quad (22)$$

Therefore, the SVC-simulated transition parameters in the validation period can be corrected with the correction factors:

$$\begin{aligned} P_{01}^{\mathrm{vali}} &= P_{01}^{\mathrm{SVC,vali}} \times \sigma \\ P_{11}^{\mathrm{vali}} &= P_{11}^{\mathrm{SVC,vali}} \times \gamma \end{aligned}. \quad (23)$$

Parameters P_{01}^{vali} and P_{11}^{vali} are the corrected transition probabilities utilized to generate the random occurrence in the validation period. The precipitation state series in the validation period is generated using the MC method and a random number:

$$W_t^{\mathrm{MC,vali}} = \begin{cases} 1 & \mathrm{rand} \le P_{11}^{\mathrm{vali}}, W_{t-1}^{\mathrm{MC,vali}} = 1 \\ 0 & \mathrm{rand} > P_{11}^{\mathrm{vali}}, W_{t-1}^{\mathrm{MC,vali}} = 1 \\ 1 & \mathrm{rand} \le P_{01}^{\mathrm{vali}}, W_{t-1}^{\mathrm{MC,vali}} = 0 \\ 0 & \mathrm{rand} > P_{01}^{\mathrm{vali}}, W_{t-1}^{\mathrm{MC,vali}} = 0 \end{cases}, \quad (24)$$

where $W_t^{\mathrm{MC,vali}}$ is the MC-simulated precipitation state on day t and rand is a uniformly distributed random number ranging from 0 to 1.

The MC-simulated precipitation state is used to correct the randomly SVC-simulated precipitation occurrence when the states generated with the MC and SVC methods in the same day t are opposite:

$$W_t = \begin{cases} W_t^{\mathrm{MC,vali}} & W_t^{\mathrm{MC,vali}} = W_t^{\mathrm{SVC,vali}} \\ W_t^{\mathrm{MC,vali}} & W_t^{\mathrm{MC,vali}} \ne W_t^{\mathrm{SVC,vali}}, \mathrm{rand} \le \mathrm{threshold} \\ W_t^{\mathrm{SVC,vali}} & W_t^{\mathrm{MC,vali}} \ne W_t^{\mathrm{SVC,vali}}, \mathrm{rand} > \mathrm{threshold} \end{cases}, \quad (25)$$

where W_t is the final simulated objective precipitation state on day t and threshold is a number ranging from 0 to 1 defined by the user. When threshold is 0, W is a completely SVC-simulated series, while when threshold is 1, W is a completely MC-simulated series. In this study, threshold = 0.7.

After the generation of precipitation occurrences, the precipitation amount is then simulated using the SVM regression algorithm. The statistical regression relationship between observed data and NCEP–NCAR predictors was constructed on wet days:

$$R_t^{\mathrm{obs}} = F_{\mathrm{SVR}}(u_t^1, u_t^2, \ldots, u_t^j) \quad w_t^{\mathrm{obs}} = 1. \quad (26)$$

Finally, the precipitation series was generated with a residual term added to each precipitation amount on wet days to fit the precipitation variance:

$$\begin{cases} R_t^{\mathrm{sim}} = F_{\mathrm{SVR}}(\widehat{u_t^1}, \widehat{u_t^2}, \ldots, \widehat{u_t^j}) + e & W_t = 1 \\ R_t^{\mathrm{sim}} = 0 & W_t = 0 \end{cases}. \quad (27)$$

c. *Evaluation of the results*

Maraun et al. (2010) suggested some useful statistics for evaluating precipitation downscaling. The statistics of downscaling results, which can represent intensity, temporal and spatial characteristics, and metrics, characterize the relevant physical processes that are used in evaluating the effect of downscaling, such as the mean value, variance, and quantiles for quantizing the precipitation distribution. H. Chen et al. (2012) found that the accuracy of a statistical downscaling model cannot be completely proven, even for cases in which

TABLE 1. Definitions of the indicators for evaluating the statistical downscaling methods.

Indicators	Definition	Major influence factor
Mean	Average of all values	Amount
Standard deviation	Standard deviation of all values in each time period	Amount and occurrence
Percentile 95	Value of the user specified percentile	Amount and occurrence
5-day maximum precipitation	Annual maximum total accumulated over 5 days	Amount and occurrence
Percentage wet	Percentage of days that exceed the wet-day threshold	Occurrence
Maximum dry spell length	Annual maximum spell with amounts less than the wet-day threshold	Occurrence
Maximum wet spell length	Annual maximum spell with amounts greater than or equal to the wet-day threshold	Occurrence
Average dry spell length	Annual average spell with amounts less than the wet-day threshold	Occurrence
Average wet spell length	Annual average spell with amounts greater than or equal to the wet-day threshold	Occurrence

the most widely used statistics in the literature for evaluating statistical downscaling methods show a good performance.

In this study, meteorological statistics, including seasonal and annual mean value, standard deviation, 95th percentile value, 5-day maximum precipitation, percentage wet, average dry spell length, average wet spell length, maximum dry spell length, maximum wet spell length (details in Table 1), relative error (RE), and relative root-mean-square error (RRMSE) were calculated and utilized to verify fitness between simulations and observations.

Of these meteorological statistics, percentage wet, average dry spell length, maximum dry spell length, average spell length, and maximum wet spell length are influenced only by precipitation occurrence. From these five statistics, the performance of downscaling precipitation occurrence can be examined. The mean value is influenced only by the amount simulation. Both occurrence and precipitation amount downscaling influence the remaining statistics. In this study, the monthly mean value was used to evaluate the RE and analyze the effect of precipitation amount simulation.

RE is calculated using the following equation:

$$\mathrm{RE} = \frac{\overline{R}_{\mathrm{sim}} - \overline{R}_{\mathrm{obs}}}{\overline{R}_{\mathrm{obs}}}, \tag{28}$$

where $\overline{R}_{\mathrm{sim}}$ is the average of a simulated precipitation series and $\overline{R}_{\mathrm{obs}}$ is the average of an observed precipitation series.

RRMSE is calculated using the following equation:

$$\mathrm{RRMSE} = \sqrt{\frac{1}{n}\sum_{i=1}^{n}\left(\frac{R^i_{\mathrm{sim}} - R^i_{\mathrm{obs}}}{R^i_{\mathrm{obs}}}\right)} \times 100\%, \tag{29}$$

where n is the total number of months in the given precipitation series, R^i_{obs} is the ith month observed precipitation, and R^i_{sim} is the ith month simulated precipitation.

In this study, the proposed methods were compared to SDSM. To further examine the differences between statistical downscaling methods in terms of generating precipitation given climate model outputs, the above evaluation criteria were first applied to precipitation generated from the GCM for the historical record (1965–2005). Then, using each method, GCMs provided simulated future (2031–2100) precipitation to evaluate the effects of future climate change under two emission scenarios. Because the R-LD method cannot simulate extreme precipitation well, it is not considered in the future maximum precipitation simulation.

3. Study region and data

To verify simulations using the proposed downscaling model, the upper Xiangjiang River basin in China was selected as a case study. The corresponding gridded NCEP and GCM output variables were the input predictors for the downscaling methods. Observed site-specific precipitation was used to evaluate the performance of the proposed model.

a. Study region

The Xiangjiang River basin in China, ranging between 24°31′ and 29°00′N and 110°31′ and 114°00′E, as shown in Fig. 2, is one of the principal tributaries to the Yangtze River. It has a drainage area of 94 660 km^2 and is 856 km long with an average land slope of 0.134‰. The upper part of the Xiangjiang River basin, which has an area of 52 150 km^2, has been selected to perform the study.

For the historical period, the mean annual air temperature of the Xiangjiang basin was 17°C. The minimum temperature is about 4°–8°C in January, and maximum temperature was about 29°–30°C in July. The mean annual precipitation is 1300–1700 mm, increasing from south to north, and average annual evapotranspiration

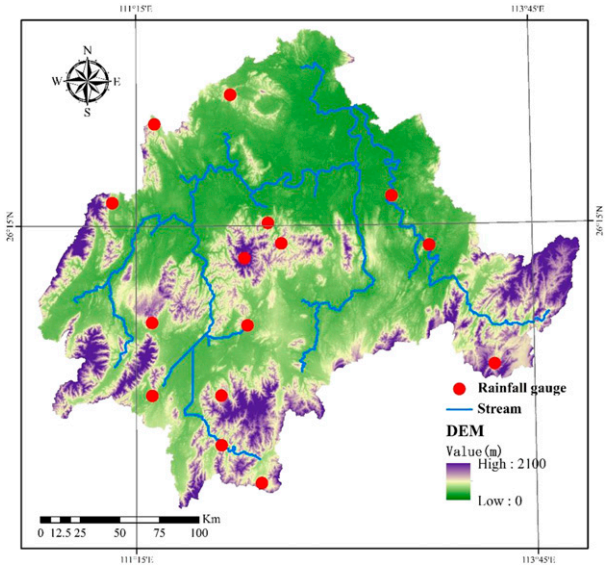

FIG. 2. Location of the upper Xiangjiang River basin and selected weather stations.

is about 641 mm (Xu et al. 2013). Nearly 80% of the incidents of extreme precipitation in the Xiangjiang basin last less than a day, and most occur in June, July, and August. Recently, the intensity and frequency of extreme precipitation have shown an increasing trend, which makes the accurate prediction of precipitation in this basin even more important.

b. Data

Fifteen hydrometeorological stations in the upper Xiangjiang River basin with daily-observed precipitation from 1965 to 2014 were used in this study. All stations have a complete series of precipitation with no missing data. Two types of calibration and validation period combinations were used for the downscaling. One uses the period from 1965 to 1990 for calibration and 1991–2005 for validation (sequential split sample), and the other uses odd-numbered years of the whole time period for calibration and even-numbered years for validation (odd–even-year split sample). Moreover, the period from 2006 to 2014 is selected as the mutual testing period to evaluate the performance of both calibration methods. The odd–even-year division reduces the influence of possible climatic changes caused by human activity. NCEP reanalysis data, with a resolution of 2.5° × 2.5° in longitude and latitude, were used as predictors to calibrate and validate the statistical relationship with the observed data using different downscaling methods during the historical period.

The output variables from the BCC_CSM RCP4.5 and RCP8.5 were utilized as predictors to simulate future climate change. These GCMs belong to the fifth phase of the Coupled Model Intercomparison Project (CMIP5), which aims to provide essential data to study climate change in the IPCC AR5 assessment process (Taylor et al. 2012). In CMIP5, representative concentration pathways (RCPs) represent possible future emission scenarios. RCP8.5 represents a high-emission environment, while RCP4.5 simulates a medium-emission environment (van Vuuren et al. 2011).

The initial gridded variables, which represent the spatial resolution in a large-scale grid, cannot completely represent station-scale data. Therefore, prior to using them as the inputs to the downscaling models, all chosen factors in the NCEP data in the nearest nine grids were interpolated into point-scale data at each station using the inverse distance weighted method (Gemmer et al. 2004) to improve their representativeness.

4. Results and discussion

In this proposed MC-LD method, precipitation occurrence was generated using the SVC and MC, calibrated using the precipitation states in the observed data. The statistical relationship between the observed precipitation series and NCEP reanalysis factors on wet days, in terms of the precipitation magnitude, was constructed using the SVM in the calibration period. That relationship was then used to simulate the precipitation series for the validation period. To reduce the number of calculations, large-scale climate variables extracted from the NCEP reanalysis data were screened; the correlations between each of the factors and the observed series were ranked with the correlation coefficient threshold for each factor set to 0.25. The filtered climate factors used in the downscaling methods are sea level pressure (mslpgl), geopotential height at 500 hPa (p500gl), specific humidity at 850 hPa (p8_sgl), wind speed at 500 hPa (p5_fgl), air temperature at 850 hPa (p8_tgl), and surface air temperature (tempgl). Two types of calibration and validation periods were used to construct the three statistical downscaling methods and their results are compared in the following sections.

a. Evaluation of uncertainty caused by optimized parameters in SVM

Before comparing the performance of multiple downscaling methods, the uncertainty brought because of SVM must be evaluated. In SVM, the regularization parameter C and kernel bandwidth σ are two parameters that required adjusting. As these two parameters are used as a whole, the values of the parameters directly determine the SVM training and generalization performance. The parameter C describes the balance between the maximum classifier boundary and classifier error in

the training process. A larger value of C produces a more accurate classified result in the training dataset; however, the generalization ability will decline with larger values of C. When using the RBF kernel function, σ can control the width of the RBF kernel; if σ gets too big, the RBF kernel performance becomes similar to that of a first-order polynomial kernel, losing the advantage of the RBF kernel status. An optimization method is required to derive suitable parameters, which may also cause overfitting. To avoid the overfitting problem, we utilized the iteratively reweighted SVM, an effective technique to improve the robustness of SVM by reweighting the samples to reduce the negative influence of the abnormal samples. The grid search method and leave-one-out cross-validation method were used to optimize the parameters and construct the cost function of optimization. We defined the range in C and σ as 1–50, which prevents the parameters from reaching the minimum or maximum value.

Because of the randomness in the parameter optimization algorithm, the sets of SVM parameters can vary with different runs, even with the same inputs. Figure 3 shows the fluctuation in parameters of the regression and classification results using the CR-LD method with 100 runs in June in the flood season. As shown in the figure, the values of C and σ have a relatively stable variance with multiple simulations, and there are few cases where parameters reach extreme values, which proves the robustness of the SVM in this case study.

b. *Comparison of precipitation occurrence simulations*

The statistics from 15 stations were averaged to represent area mean values. As all stations are from neighboring areas and have strong relationships, the comparison between the results of the closest 15 stations is conducted to reflect regional uncertainty analysis. Tables 2 and 3 present the total average statistics of observed and downscaled precipitation using different downscaling methods with two types of calibration and validation periods [i.e., sequential split-sample method (Table 2) versus odd–even-year split-sample method (Table 3) proposed in this study].

A statistic in bold font indicates that the corresponding method performs better than other methods in the table. Nine statistics were evaluated at an annual time scale. All statistics were divided into two categories, which are related to amounts (mean, standard deviation, 95th percentile, and 5-day maximum precipitation) and occurrences (percentage wet, maximum dry spell length, maximum wet spell length, average dry spell length, and average wet spell length). With the sequential split-sample method, the MC-LD, CR-LD,

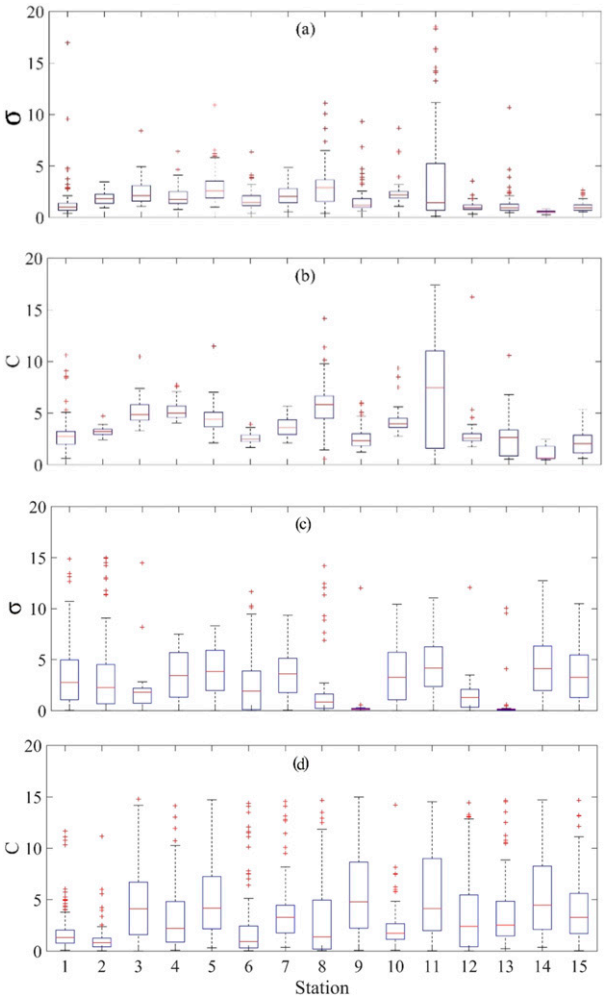

FIG. 3. Box plots of the SVM parameters in the CR-LD method with 100 runs in June as the calibration period and using the sequential split-sample method at 15 stations, (a),(b) SVR and (c),(d) SVC. Panels (a) and (c) indicate variations in the C parameter and (b) and (d) indicate variations in the σ parameter.

and SDSM resulted in smaller errors for more of the statistical parameters in the calibration period than R-LD. MC-LD performed better than SDSM according to the percentage wet and maximum and average wet spell length, while SDSM performed better than MC-LD in maximum dry spell lengths. Over the validation period, MC-LD showed a slight advantage over SDSM in most statistical comparisons; generally, MC-LD performed better than SDSM in reproducing the precipitation occurrence in the calibration period. In both periods, CR-LD produced slightly less accurate statistics than those from MC-LD. In addition, CR-LD showed a substantial disadvantage in terms of dry and wet spell lengths. Using the odd–even-year split-sample method (odd-numbered years for calibration and even-numbered years for validation) resulted in

TABLE 2. Mean annual statistics for meteorological stations in the Xiangjiang River basin using the sequential split-sample method. The value in bold font indicates that the corresponding method performs better than other methods in the table.

Indicators	Calibration period (1965–90)					Validation period (1991–2005)				
	Obs.	MC-LD	SDSM	CR-LD	R-LD	Obs.	MC-LD	SDSM	CR-LD	R-LD
Mean (mm)	4.19	3.6	4.83	3.44	**3.77**	3.99	**3.79**	4.87	3.71	3.78
Standard deviation (mm)	10.5	9.07	**9.17**	8.81	3.46	9.93	**9.75**	9.25	9.64	2.99
Percentile 95 (mm)	23.84	20.74	**25.49**	19.79	10.54	22.65	**21.88**	25.46	21.55	8.82
5-day maximum precipitation (mm)	163.18	158.38	130.59	**167.27**	62.67	154.05	**173.9**	127.09	185.84	56.76
Percentage wet	0.41	**0.39**	0.35	0.65	0.75	0.4	**0.39**	0.34	0.37	0.91
Maximum dry spell length (days)	25.61	19.96	22.64	37.44	**22.9**	24.87	18.61	19.09	**28.39**	3.61
Maximum wet spell length (days)	11.34	**10.1**	8	14.65	60.36	10.76	**10.26**	7.4	13.35	183.16
Average dry spell length (days)	4.05	**3.91**	3.69	5.81	3.6	4.04	**3.94**	3.46	4.94	1.06
Average wet spell length (days)	2.82	**2.51**	1.99	3.51	14.14	2.76	2.52	1.78	**2.93**	15.5
RE (%)	—	**−0.78**	24.73	−7.93	−7.92	—	−14.22	15.27	−17.93	**−10.11**
RRMSE (%)	—	41.41	54.55	57.12	**37.59**	—	63.82	72.96	74.38	**63.33**

similar accuracies between the downscaling methods compared with those produced from the sequential split-sample method. The exception was that MC-LD had an obviously better standard deviation and 5-day maximum precipitation performance using the split-sample calibration–validation.

Based on simulated precipitation occurrence, the coupling of the support vector classifier and Markov chain approach provides a more stable performance in these indicators. This approach also provides a better performance for the SDSM and SVC occurrence generators. Comparing the performances of MC-LD, CR-LD, and R-LD, it is clear that regardless of model calibration and validation used, the R-LD method has poor ability to generate precipitation series with daily characteristics and can only generate the mean value of precipitation. The Markov chain brings an improvement over the SVC method in precipitation occurrence simulation. Meanwhile, the existence of an occurrence classifier is important for the regression method, as proven from comparisons between the R-LD and other methods.

Figure 4 shows the monthly occurrence statistics in the two types of validation periods and indicates that in both calibration types, there is little difference between MC-LD, SDSM, and CR-LD in terms of wet day predictions. However, MC-LD and SDSM outperformed CR-LD on average dry and wet spells. Compared to the other methods, without an occurrence generator, the R-LD's performance was weak for most statistical parameters.

Figure 5 shows box plots of annual statistics at all stations in the validation period. As shown, the distributions of most statistical values generated from MC-LD at different stations were closer to observations, especially in the percentage of wet days. While SDSM and CR-LD had better performances in some seasonal cases, most annual results from SDSM and CR-LD were not as good as those of MC-LD. However, there was a great mismatch between the observed and simulation precipitation from the R-LD method in most statistical values. Influenced by the lack of an occurrence generator, the R-LD method does not show a stable enough performance to simulate the spell lengths. Furthermore,

TABLE 3. As in Table 2, but for the odd–even-year split-sample method.

Indicators	Calibration period (odd years)					Validation period (even years)				
	Obs.	MC-LD	SDSM	CR-LD	R-LD	Obs.	MC-LD	SDSM	CR-LD	R-LD
Mean (mm)	3.93	3.85	4.88	3.79	3.99	3.99	3.71	5.01	3.67	3.67
Standard deviation (mm)	9.73	**9.53**	9.07	9.34	3.54	10.06	9.18	**9.2**	9.11	3.8
Percentile 95 (mm)	22.2	**21.71**	25	21.52	11.09	22.76	**21.13**	25.28	21.05	10.22
5-day maximum precipitation (mm)	147.27	172.71	**131.29**	178.98	67.32	161.1	**164.5**	132.74	179.7	78.2
Percentage wet	0.4	**0.4**	0.35	0.64	0.9	0.4	**0.39**	0.36	0.38	0.91
Maximum dry spell length (days)	25.83	19.92	**21.39**	39.09	7.12	26.43	20.25	**21.2**	38.87	5.82
Maximum wet spell length (days)	5.35	**5.58**	4.16	8.49	61.96	5.41	**5.36**	4.32	7.63	55.31
Average dry spell length (days)	4.03	**3.95**	3.63	6.12	2.31	4.2	**4.03**	3.6	6.29	2
Average wet spell length (days)	2.74	**2.65**	1.97	3.91	23.81	2.77	**2.54**	2.02	3.8	22.58
RE (%)	—	−1.86	24.18	−3.4	**1.5**	—	**7.05**	25.34	−8.09	−8.15
RRMSE (%)	—	40.81	54.05	52.75	**39.62**	—	**56.70**	62.94	68.54	60.22

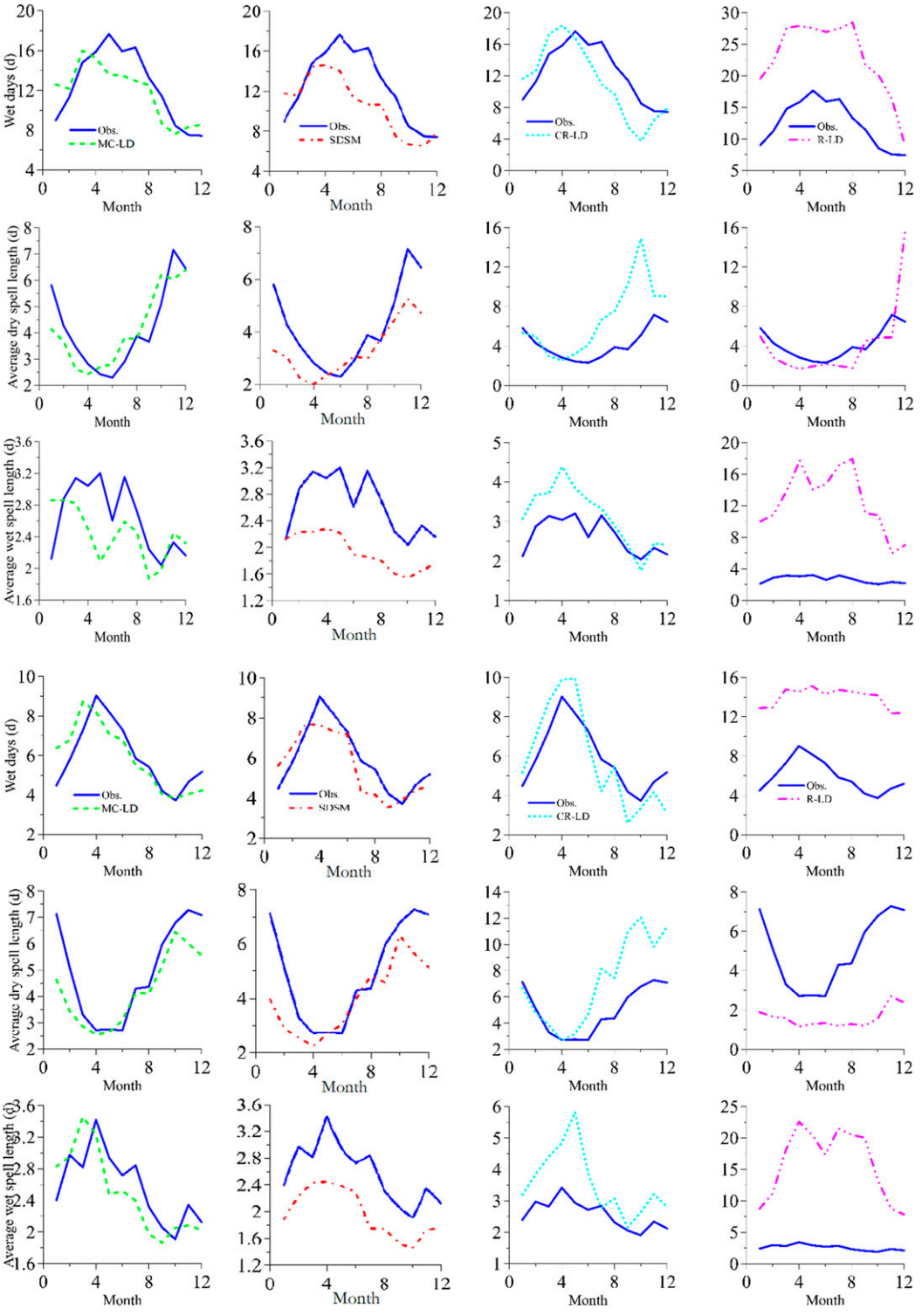

FIG. 4. (top) Monthly average statistical values for the Xiangjiang River basin resulting from downscaling using the sequential split-sample method in the validation period. (bottom) Monthly average statistical values for the Xiangjiang River basin resulting from downscaling using the odd–even-year split-sample method in the validation period.

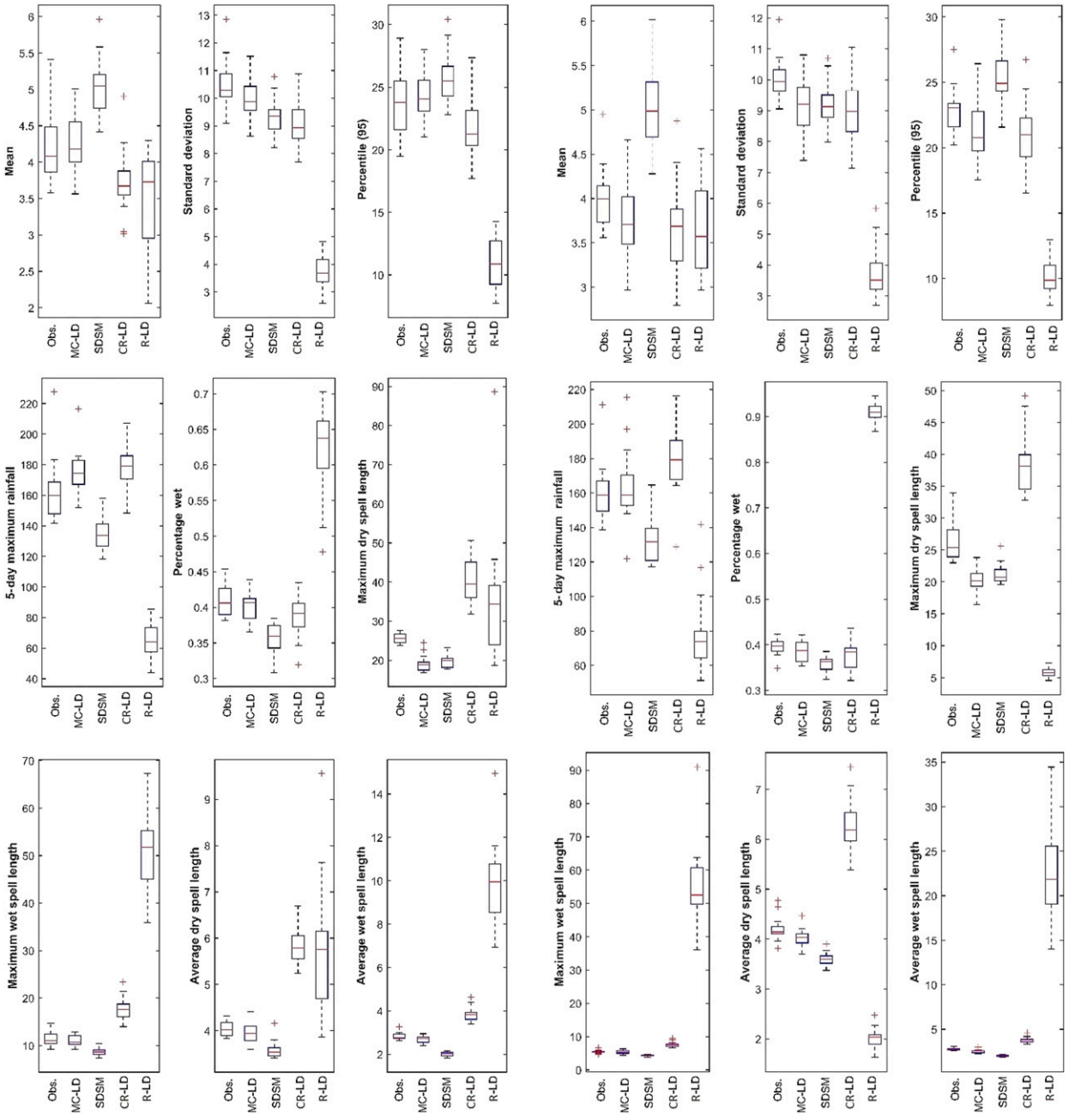

FIG. 5. (left) Box plots of annual indicators for the Xiangjiang River basin using the sequential split-sample method in the validation period. (right) Box plots of annual indicators for the Xiangjiang River basin using the odd–even-year split-sample method in the validation period.

the length of each box can explain the variance in the corresponding statistical values at all 15 stations. MC-LD values showed a similar distribution as the observations in percentage wet and average dry spell length, which proves that MC-LD described the otherness of different stations quite well. Meanwhile, there were large differences in spell lengths between the observations and R-LD calculations with both calibration methods. With the odd–even-year split-sample method, MC-LD outperformed SDSM and CR-LD in most statistical parameters. These results revealed that MC-LD was an overall significant improvement over CR-LD and R-LD.

The occurrence statistical values from MC-LD, SDSM, and CR-LD were generally satisfactory, while R-LD had poor ability to generate the occurrence.

MC-LD, meanwhile, had a better capacity to simulate the precipitation occurrence, which was not possible using SVM regression exclusively. Meanwhile, when the split-sample methods were changed, MC-LD maintained a stable performance, while SDSM did not adapt to calibrating the discontinuous data. Furthermore, lowering the disparity between the precipitation in the calibration and validation periods resulted in the MC-LD offering an even better performance.

c. *Comparison of the precipitation amount simulations*

Tables 2 and 3 represent the relative error using different downscaling methods, time periods, and calibration methods. The MC-LD, CR-LD, and R-LD methods provided better agreement with the precipitation amount than SDSM in terms of the relative error, which confirmed the reliable robustness of SVM for simulating the precipitation amount (Anandhi et al. 2008). Tables 2 and 3 indicate that there were about 10%–20% positive errors in precipitation simulated with SDSM in all cases, while the relative errors simulated with MC-LD, CR-LD, and R-LD were better than those from SDSM. There are no clear differences in the relative errors between the calibration and validation periods with both split-sample methods. In terms of the RRMSE, while none of the downscaling methods provided a completely satisfactory result, MC-LD and R-LD performed better than SDSM for both calibration methods (Tables 2 and 3), and there was no clear difference between MC-LD and R-LD. It is also clear that the simulations using the sequential split-sample validation periods performed slightly better than those using the odd-even-year split-sample method.

The precipitation amount statistics presented in Fig. 5 show that the SDSM results were closer to those of the observation in standard deviation using the sequential split-sample method, while MC-LD performed better using the odd–even-year split-sample method. However, most annual results from SDSM and CR-LD were not as good as those from MC-LD. The MC-LD method provided statistical values from different stations that were close to the observed statistical values, especially in mean value and 95 percentile. In contrast, except for the mean value, the R-LD method performed the worst.

The monthly average statistical values produced from the MC-LD, CR-LD, R-LD, and SDSM methods for two validation period types in the Xiangjiang River basin are presented in Fig. 6. Generally, MC-LD, CR-LD, and R-LD had a better agreement with the monthly mean value than SDSM, which overestimated the mean value in the first half of the year while performing relatively well in the second half. The SDSM, MC-LD, and CR-LD had relatively accurate estimations of standard deviation, while R-LD often underestimated the standard deviation. Meanwhile, the statistical values using the odd–even-year split-sample method showed an obvious improvement in 5-day maximum precipitation simulation compared to statistical values using the sequential split-sample method. The overall better performance of MC-LD can be attributed to the advantages of the nonlinear regression (SVM) over the linear regression method (SDSM).

For illustrative purposes, Fig. 7 shows the quantile–quantile plots for the daily precipitation on wet days at randomly selected stations for validation periods. The MC-LD significantly outperformed the CR-LD, followed by the SDSM, especially for precipitation greater than 50 mm day^{-1}. For precipitation amounts above 50 mm day^{-1}, the SDSM underestimated the precipitation amount, while the MC-LD and CR-LD simulations were closer to observations. The excellent agreement with observations indicated that MC-LD was a more accurate model for simulating extreme events. Overall, the R-LD regression method performed the worst. The underestimation shown in most of the percentiles may have been caused by the lack of an occurrence generator to distribute the precipitation over more wet days. In addition, in the validation period, MC-LD performed better using the odd–even-year split-sample method than using the sequential split-sample method; therefore, it can be inferred that using odd and even years for calibration and validation eliminates potential effects from trending data.

d. *Comparison of simulations using different split-sample methods*

Because the validation periods of the two split-sample methods were different, comparing the two split-sample methods was challenging. To evaluate their difference in the same time period, the period from 2006 to 2014 was selected as a test period. The area-average statistical values from all downscaling methods are shown in Tables 4 and 5.

Results indicated that all downscaling methods provided relatively stable and satisfying performance using both methods. In addition to these average statistical values, it is also meaningful to evaluate the performance in downscaling precipitation at each site. The precipitation annual average mean, standard deviation, and percentage wet values from observations and different downscaling methods at each station are shown in Fig. 8. The results indicated that each station had values similar to the regional averages in Tables 4 and 5. However,

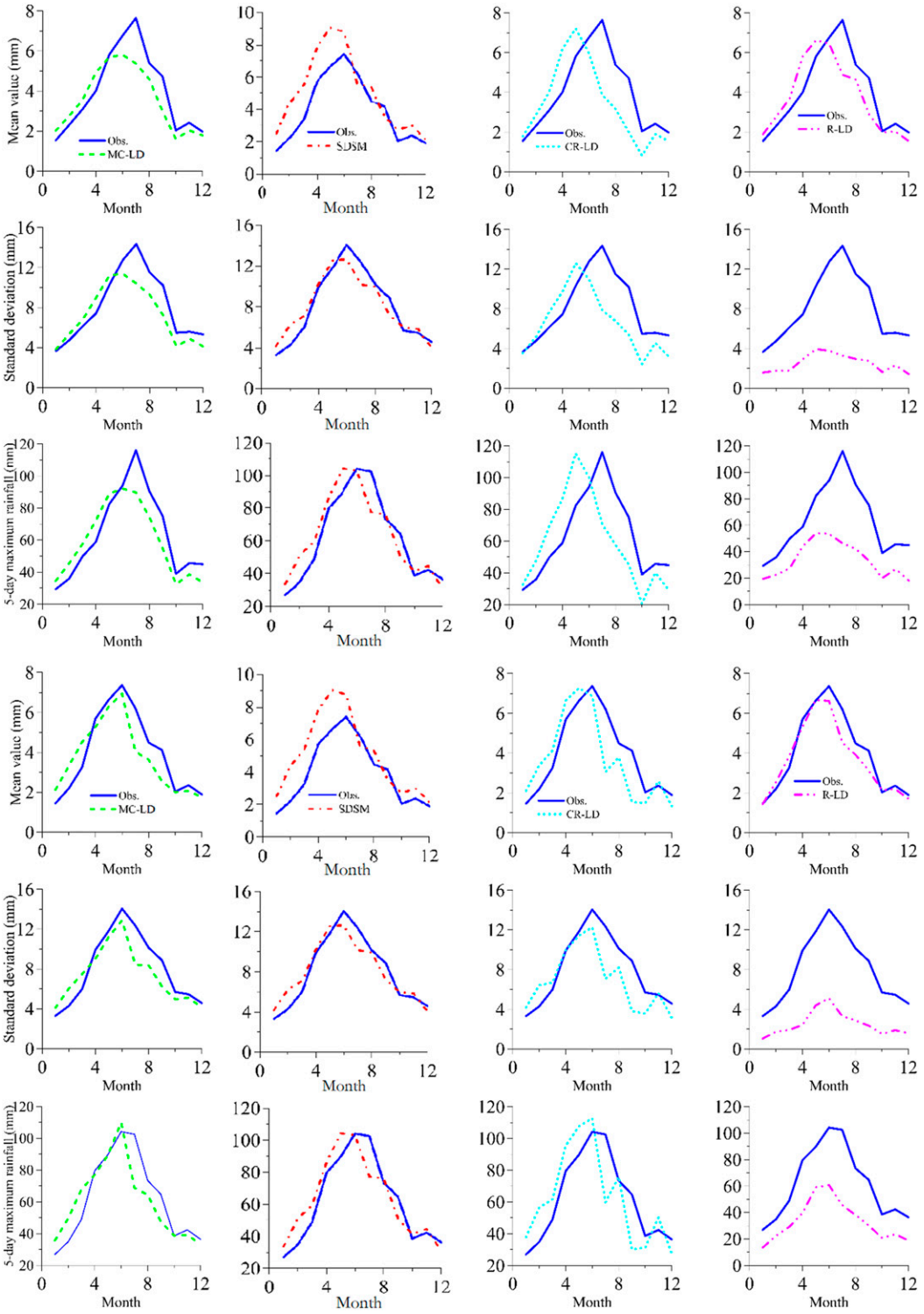

FIG. 6. (top) Monthly average statistical values for the Xiangjiang River basin influenced by both amount and occurrence of downscaling using the sequential split-sample method in the validation period. (bottom) Monthly average statistical values for the Xiangjiang River basin influenced by both amount and occurrence of downscaling using the odd–even-year split-sample method in the validation period.

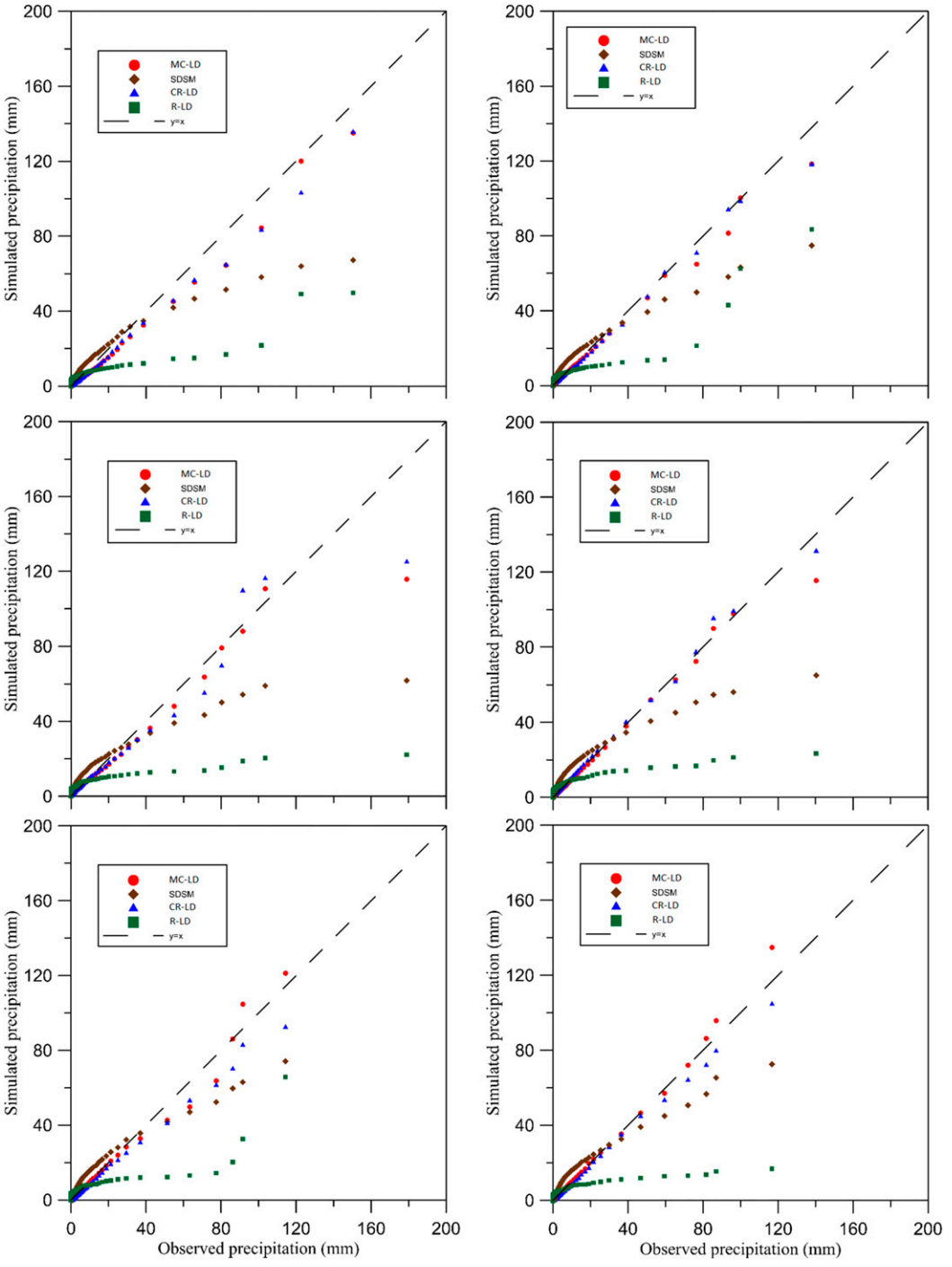

FIG. 7. Quantile-to-quantile plot for daily precipitation regression on wet days with less than 200 mm day^{-1} at selected stations using different calibrating methods in the validation period: (left) sequential split-sample method and (right) odd–even-year split-sample methods.

there was an underestimation of the standard deviation and percentage wet at most stations in the testing period. Comparing the different downscaling methods, the statistical values from the MC-LD method were closer to observations than the other downscaling methods at more stations. Among all downscaling methods, MC-LD had the best performance in the testing period. Furthermore, all downscaling methods provided stable

TABLE 4. Mean annual statistics for meteorological stations in the testing period in the Xiangjiang River basin using the sequential split-sample method. The value in bold font indicates that the corresponding method performs better than other methods in the table.

Indicators	Testing period				
	Obs.	MC-LD	SDSM	CR-LD	R-LD
Mean (mm)	3.80	**3.74**	4.39	3.21	3.70
Standard deviation (mm)	10.10	**9.48**	8.77	9.14	2.38
Percentile 95 (mm)	22.28	20.73	**24.07**	19.23	7.78
5-day maximum precipitation (mm)	165.68	**173.06**	124.41	189.56	43.54
Percentage wet	0.39	**0.36**	0.33	0.29	0.96
Maximum dry spell length (days)	25.83	**25.45**	21.15	113.65	6.30
Maximum wet spell length (days)	10.81	**7.66**	7.07	27.21	276.79
Average dry spell length (days)	4.20	**4.98**	3.57	9.09	0.81
Average wet spell length (days)	2.71	**2.96**	1.74	4.19	7.37
RE (%)	—	**−1.58**	15.53	−15.53	−2.63
RRMSE (%)	—	66.87	74.66	76.60	**64.94**

and satisfying performances using both split-sample calibration methods in the testing period.

e. *Comparison of future simulations*

The proposed downscaling methods were used to simulate changes in future precipitation. Historical precipitation simulated using a GCM and different downscaling methods are compared to the observed series in Table 6.

For historical simulations, MC-LD performed better than the other methods according to the evaluation parameters using both types of calibration methods. It was observed that changing the predictors (from NCEP to GCM historical) had an influence on the SDSM occurrence generator; MC-LD was more accurate when using different predictors as the model input.

Changes in annual mean precipitation in the medium-term future (2031–60) and long-term future (2071–2100) periods compared to the historical period (1971–2000) are shown in Fig. 9. The results indicated increasing trends in future precipitation from all model simulations at most stations. For the medium future, the precipitation did not show a clear increase, except for the precipitation generated from SDSM in the RCP8.5 scenario. Furthermore, there was no clear difference generated between different emission scenarios for the medium-term future. However, in the long-term future, precipitation derived from all methods showed a positive increasing trend, and mean precipitation and variability in the RCP8.5 scenario was significantly larger than in the RCP4.5 scenario.

Influenced by the East Asian subtropical monsoon, the monsoon period of the Xiangjiang River basin falls mainly in June and July. Similar to annual precipitation, in the monsoon season, there was a slight increase in precipitation as derived from all methods, with less fluctuation at different stations in the medium-term future. For the long-term future, distinct increasing trends were found, and variations in mean precipitation in the RCP8.5 scenario were clearly larger than those in RCP4.5 scenario. Generally, the monsoon season has smaller increasing trends and variability in precipitation than the annual totals.

TABLE 5. As in Table 4, but for the odd–even-year split-sample method.

Indicators	Testing period				
	Obs.	MC-LD	SDSM	CR-LD	R-LD
Mean (mm)	3.80	3.55	4.57	3.20	**3.93**
Standard deviation (mm)	10.10	**9.38**	8.87	8.95	3.03
Percentile 95 (mm)	22.28	**20.92**	24.42	19.32	9.55
5-day maximum precipitation (mm)	165.68	**168.57**	118.42	172.54	60.29
Percentage wet	0.39	**0.35**	0.33	0.31	0.95
Maximum dry spell length (days)	25.83	**20.70**	19.20	42.41	8.41
Maximum wet spell length (days)	10.81	**9.41**	6.90	12.59	260.95
Average dry spell length (days)	4.20	**4.06**	3.53	6.33	2.45
Average wet spell length (days)	2.71	**2.27**	1.71	2.97	10.91
RE (%)	—	−6.58	20.26	−15.79	**3.42**
RRMSE (%)	—	**63.15**	71.50	77.58	65.53

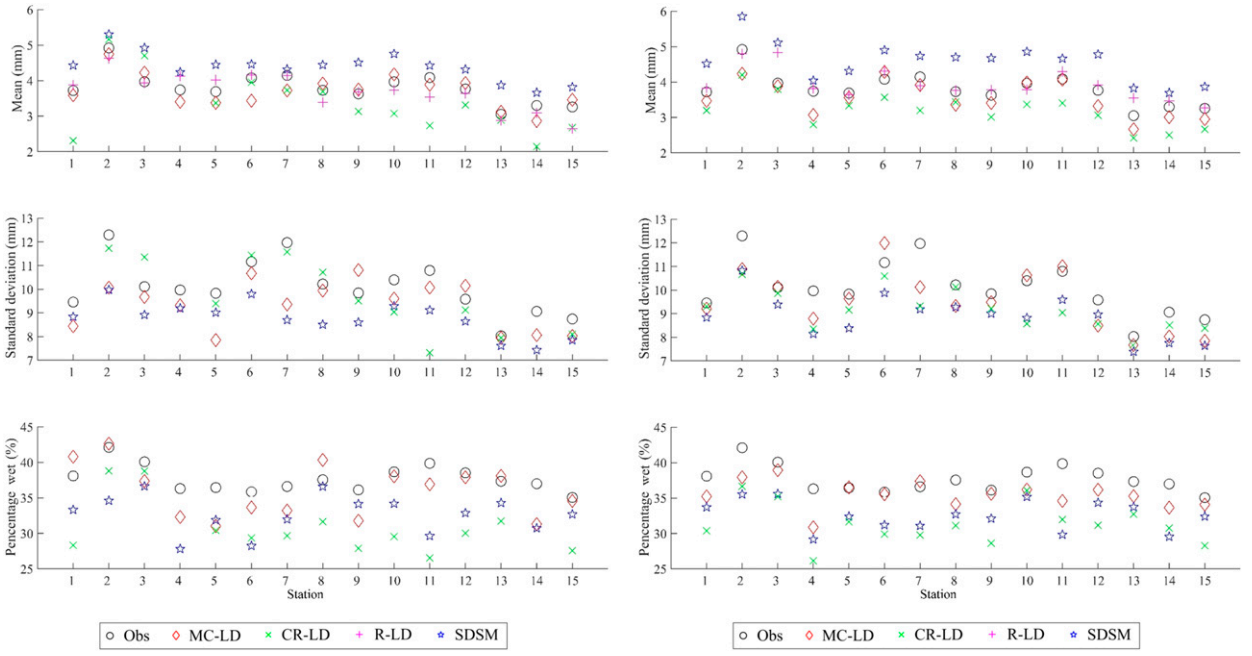

FIG. 8. (left) Evaluation statistical values for each station using the sequential split-sample period in the testing period. (right) Evaluation statistical values for each station using the odd–even-year split-sample period in the testing period.

Extreme events determine the extent taken in preventive measures as communities anticipate future floods. Therefore, extreme events play a crucial role in the economy and environment and must be evaluated. From the trend in annual maximum precipitation from 2031 to 2100 in Fig. 9, future precipitation at most stations and all downscaling methods and scenarios showed positive trends. With respect to the RCP8.5 scenario, the precipitation generated from statistical downscaling methods at 15 stations showed higher amplitude variations than the RCP4.5 scenario. Furthermore, the MC-LD results from the RCP8.5 scenario showed a more conservative trend and larger fluctuations than the CR-LD and SDSM predictions.

5. Conclusions

This study presented a revised regression-based statistical downscaling method coupling a first-order, two-state Markov chain and least squares support vector machine developed to improve the performance of statistical downscaling methods. The following conclusions were drawn:

1) A comparison of precipitation occurrence simulations from the MC-LD, CR-LD, and SDSM methods showed that the first-order Markov chain provides a better performance to SVC in precipitation occurrence frequency simulation, such as percentage wet

TABLE 6. Mean annual statistics for the meteorological stations in the Xiangjiang River basin with GCM historical indicators as input (1965–2005). The value in bold font indicates that the corresponding method performs better than other methods in the table.

Indicators	Sequential split sample					Odd–even-year split sample				
	Obs.	MC-LD	SDSM	CR-LD	R-LD	Obs.	MC-LD	SDSM	CR-LD	R-LD
Mean (mm)	3.99	**3.79**	4.87	3.71	3.78	3.99	3.8	4.97	**3.83**	3.66
Standard deviation (mm)	9.93	**9.75**	9.25	9.64	2.99	9.93	9.84	9.23	**9.86**	3.5
Percentile 95 (mm)	22.65	**21.88**	25.46	21.55	8.82	22.65	21.78	25.56	**22.19**	10.06
5-day maximum precipitation(mm)	154.05	**173.9**	127.09	185.84	56.76	154.05	174.35	**133.84**	190.8	70.15
Percentage wet	0.4	**0.39**	0.34	0.37	0.96	0.4	**0.38**	0.35	0.37	0.91
Maximum dry spell length (days)	24.87	18.61	19.09	**28.39**	3.61	24.87	19.09	**23.12**	36.2	6.02
Maximum wet spell length (days)	10.76	**10.26**	7.4	13.35	183.16	10.76	**9.89**	9.3	15.83	108.56
Average dry spell length (days)	4.04	**3.94**	**3.46**	4.94	1.06	4.04	**3.93**	3.85	6.08	1.99
Average wet spell length (days)	2.76	2.52	1.78	**2.93**	15.5	2.76	**2.43**	2.12	3.63	20.57
RE compared with Obs. (%)	—	**−4.93**	22.01	−6.91	−5.21	—	−4.72	24.45	**−4.06**	−8.39
RE compared with NCEP simulation (%)	—	2.65	**1.04**	6.42	3.08	—	0.89	**0.19**	2.93	−3.6

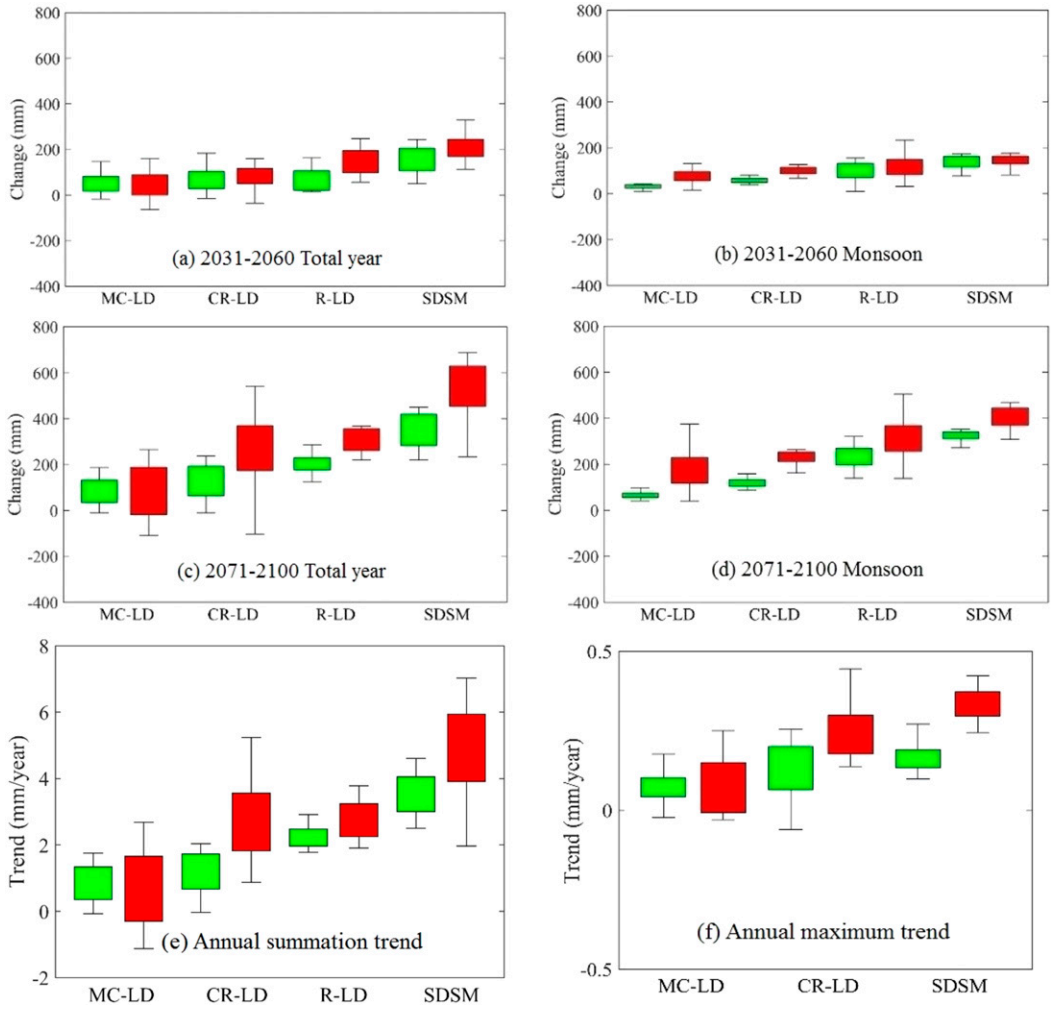

FIG. 9. Box plots of the change in mean future precipitation in (a),(b) the medium-term future (2031–60) and (c),(d) the long-term future (2071–2100) compared with the observed precipitation in the historical period (1971–2000) at 15 stations. (e),(f) Box plots of trends in annual total and maximum precipitation in the future (2031–2100). Green boxes are RCP4.5 and red boxes are RCP8.5.

days and wet spell length. With an efficient precipitation occurrence classifier, MC-LD overcame the disadvantages of a simple SVM and provided a better occurrence simulation than CR-LD. In addition, MC-LD performed better than the SDSM in most of the meteorological statistical parameters for precipitation in the Xiangjiang River basin.

2) Based on a comparison of the MC-LD and R-LD methods, the simple regression method was generally good at simulating precipitation amounts over long time scales without concentrating on the daily variance. However, with a precipitation classifier and random residual term, MC-LD well represented the temporal structure of precipitation while maintaining accurate large-scale amount simulations. The results prove that the MC-LD method utilized the advantages of the Markov chain, SVC, and SVR, facilitating better agreement with observed daily series than the SDSM.
3) It can be inferred that by reducing the impact of the climatic variation, the evaluation using the odd–even-year split-sample method made the simulations more accurate than using the sequential-years method as the calibration period, especially for MC-LD. These results also showed that MC-LD was more suitable than SDSM for handling cases with missing data from precipitation observations or otherwise fragmented data.
4) In terms of future precipitation simulations, all methods showed a similar increasing precipitation trend in the Xiangjiang River basin, with a greater variance and larger growth represented in scenario

RCP8.5 compared to scenario RCP4.5. The trends for maximum precipitation indicated the future will be characterized by more extreme precipitation events and higher abundances of available water resources.

5) Notably, the proposed MC-LD method is an at-site statistical downscaling method, which may be limited in describing intersite correlation structures of observed precipitation in neighboring locations. In future work, it would be meaningful to extend this method to multisite domains for a wider range of hydrological applications.

This study also proposes that researchers will develop more effective regression-based downscaling methods by combining different types of precipitation occurrence classifiers with regression or distribution methods. More combinations should be tested and evaluated to advance a more reasonable theory of downscaling in future research.

Acknowledgments. This research was funded by the National Natural Science Foundation of China (51339004, 51539009, and 51279138) and the Fundamental Research Funds for the Central Universities (2015206020201). The authors wish to extend their appreciation to the Earth System Research Laboratory for the NCEP data and to the Beijing Climate Center for the BCC data.

REFERENCES

Aksornsingchai, P., and C. Srinilta, 2011: Statistical downscaling for rainfall and temperature prediction in Thailand. *Proc. Int. Multiconf. of Engineers and Computer Scientists 2011*, Vol. I, Hong Kong, China, International Association of Engineers, 356–361. [Available online at http://www.iaeng.org/publication/IMECS2011/IMECS2011_pp356-361.pdf.]

Anandhi, A., V. V. Srinivas, R. S. Nanjundiah, and D. N. Kumar, 2008: Downscaling precipitation to river basin in India for IPCC SRES scenarios using support vector machine. *Int. J. Climatol.*, **28**, 401–420, doi:10.1002/joc.1529.

Awan, U. K., U. W. Liaqat, M. H. Choi, and A. Ismaeel, 2016: A SWAT modeling approach to assess the impact of climate change on consumptive water use in Lower Chenab Canal area of Indus basin. *Hydrol. Res.*, **47**, 1025–1037, doi:10.2166/nh.2016.102.

Boé, J., L. Terray, and F. Habets, 2007: Statistical and dynamical downscaling of the Seine basin climate for hydro-meteorological studies. *Int. J. Climatol.*, **27**, 1643–1655, doi:10.1002/joc.1602.

Breinl, K., T. Turkington, and M. Stowasser, 2015: Simulating daily precipitation and temperature: A weather generation framework for assessing hydrometeorological hazards. *Meteor. App.*, **22**, 334–347, doi:10.1002/met.1459.

Bürger, G., and Y. Chen, 2005: Regression-based downscaling of spatial variability for hydrologic applications. *J. Hydrol.*, **311**, 299–317, doi:10.1016/j.jhydrol.2005.01.025.

Chen, H., J. Guo, W. Xiong, S. Guo, and C. Y. Xu, 2010: Downscaling GCMs using the smooth support vector machine method to predict daily precipitation in the Hanjiang Basin. *Adv. Atmos. Sci.*, **27**, 274–284, doi:10.1007/s00376-009-8071-1.

——, C.-Y. Xu, and S. Guo, 2012: Comparison and evaluation of multiple GCMs, statistical downscaling and hydrological models in the study of climate change impacts on runoff. *J. Hydrol.*, **434–435**, 36–45, doi:10.1016/j.jhydrol.2012.02.040.

Chen, J., and F. P. Brissette, 2014: Comparison of five stochastic weather generators in simulating daily precipitation and temperature for the loess plateau of china. *Int. J. Climatol.*, **34**, 3089–3105, doi:10.1002/joc.3896.

——, ——, and R. Leconte, 2011: Uncertainty of downscaling method in quantifying the impact of climate change on hydrology. *J. Hydrol.*, **401**, 190–202, doi:10.1016/j.jhydrol.2011.02.020.

——, ——, ——, and A. Caron, 2012a: A versatile weather generator for daily precipitation and temperature. *Trans. ASABE*, **55**, 895–906, doi:10.13031/2013.41522.

——, ——, and ——, 2012b: Coupling statistical and dynamical methods for spatial downscaling of precipitation. *Climatic Change*, **114**, 509–526, doi:10.1007/s10584-012-0452-2.

——, ——, C. Diane, and B. Marco, 2013: Finding appropriate bias correction methods in downscaling precipitation for hydrologic impact studies over North America. *Water Resour. Res.*, **49**, 4187–4205, doi:10.1002/wrcr.20331.

——, X. J. Zhang, and F. P. Brissette, 2014a: Assessing scale effects for statistically downscaling precipitation with GPCC model. *Int. J. Climatol.*, **34**, 708–727, doi:10.1002/joc.3717.

——, F. P. Brissette, and R. Leconte, 2014b: Assessing regression-based statistical approaches for downscaling precipitation over North America. *Hydrol. Processes.*, **28**, 3482–3504, doi:10.1002/hyp.9889.

——, B. G. St-Denis, F. Brissette, and P. Lucas-Picher, 2016: Using natural variability as a baseline to evaluate the performance of bias correction methods in hydrological climate change impact studies. *J. Hydrometeor.*, **17**, 2155–2174, doi:10.1175/JHM-D-15-0099.1.

——, H. Chen, and S. Guo, 2017: Multi-site precipitation downscaling using a stochastic weather generator. *Climate Dyn.*, doi:10.1007/s00382-017-3731-9, in press.

Chen, S. T., P.-S. Yu, and Y.-H. Tang, 2010: Statistical downscaling of daily precipitation using support vector machines and multivariate analysis. *J. Hydrol.*, **385**, 13–22, doi:10.1016/j.jhydrol.2010.01.021.

Cheng, C. S., G. Li, and Q. Li, 2010: A synoptic weather typing approach to simulate daily rainfall and extremes in Ontario, Canada: Potential for climate change projections. *J. Appl. Meteor. Climatol.*, **49**, 845–866, doi:10.1175/2010JAMC2016.1.

Chu, J. T., J. Xia, and C. Y. Xu, 2010: Statistical downscaling of daily mean temperature, pan evaporation and precipitation for climate change scenarios in Haihe River, China. *Theor. Appl. Climatol.*, **99**, 149–161, doi:10.1007/s00704-009-0129-6.

Crane, R. G., and B. C. Hewitson, 1998: Doubled CO_2 precipitation changes for the Susquehanna basin: Down-scaling from the genesis general circulation model. *Int. J. Climatol.*, **18**, 65–76, doi:10.1002/(SICI)1097-0088(199801)18:1<65::AID-JOC222>3.0.CO;2-9.

Diaz-Nieto, J., and R. L. Wilby, 2005: A comparison of statistical downscaling and climate change factor methods: Impacts on low flows in the River Thames, United Kingdom. *Climatic Change*, **69**, 245–268, doi:10.1007/s10584-005-1157-6.

Dibike, Y., and P. Coulibaly, 2005: Hydrologic impact of climate change in the Saguenay watershed: Comparison of downscaling methods and hydrologic models. *J. Hydrol.*, **307**, 145–163, doi:10.1016/j.jhydrol.2004.10.012.

Gemmer, M., S. Becker, and T. Jiang, 2004: Observed monthly precipitation trends in China 1951–2002. *Theor. Appl. Climatol.*, **77**, 39–45, doi:10.1007/s00704-003-0018-3.

Ghosh, S., 2010: SVM-PGSL coupled approach for statistical downscaling to predict rainfall from GCM output. *J. Geophys. Res.*, **115**, 1842–1851, doi:10.1029/2009JD013548.

——, and P. P. Mujumdar, 2008: Statistical downscaling of GCM simulations to streamflow using relevance vector machine. *Adv. Water Resour.*, **31**, 132–146, doi:10.1016/j.advwatres.2007.07.005.

Giorgi, F., and Coauthors, 2001: Regional climate information—Evaluation and projections. *Climate Change 2001: The Scientific Basis*, Cambridge University Press, 583–638.

Gregory, J. M., T. M. L. Wigley, and P. D. Jones, 1993: Application of Markov models to area-average daily precipitation series and interannual variability in seasonal totals. *Climate Dyn.*, **8**, 299–310, doi:10.1007/BF00209669.

Hassan, Z., S. Shamsudin, and S. Harun, 2014: Application of SDSM and LARS-WG for simulating and downscaling of rainfall and temperature. *Theor. Appl. Climatol.*, **116**, 243–257, doi:10.1007/s00704-013-0951-8.

Hessami, M., P. Gachon, T. B. M. J. Ouarda, and A. St-Hilaire, 2008: Automated regression-based statistical downscaling tool. *Environ. Modell. Software*, **23**, 813–834, doi:10.1016/j.envsoft.2007.10.004.

Hewitson, B. C., and R. G. Crane, 2002: Self-organizing maps: Applications to synoptic climatology. *Climate Res.*, **22**, 13–26, doi:10.3354/cr022013.

Jacobeit, J., E. Hertig, S. Seubert, and K. Lutz, 2014: Statistical downscaling for climate change projections in the Mediterranean region: Methods and results. *Reg. Environ. Change*, **14**, 1891–1906, doi:10.1007/s10113-014-0605-0.

Katz, R. W., 1981: On some criteria for estimating the order of a Markov chain. *Technometrics*, **23**, 243–249, doi:10.2307/1267787.

Khan, M. S., P. Coulibaly, and Y. Dibike, 2006: Uncertainty analysis of statistical downscaling methods. *J. Hydrol.*, **319**, 357–382, doi:10.1016/j.jhydrol.2005.06.035.

Kilsby, C. G., P. D. Jones, A. Burton, A. C. Ford, H. J. Fowler, and C. Harpham, 2007: A daily weather generator for use in climate change studies. *Environ. Modell. Software*, **22**, 1705–1719, doi:10.1016/j.envsoft.2007.02.005.

Li, Y. L., H. Tso, J. Yao, and Q. Zhang, 2016: Application of a distributed catchment model to investigate hydrological impacts of climate change within Poyang Lake catchment (China). *Hydrol. Res.*, **47**, 120–135, doi:10.2166/nh.2016.234.

Liu, C. M., W. B. Liu, G. B. Fu, and R. L. Ouyang, 2012: A discussion of some aspects of statistical downscaling in climate impacts assessment (in Chinese). *Adv. Water Sci.*, **23**, 427–437.

Mandal, S., R. K. Srivastav, and S. P. Simonovic, 2016: Use of beta regression for statistical downscaling of precipitation in the Campbell River basin, British Columbia, Canada. *J. Hydrol.*, **538**, 49–62, doi:10.1016/j.jhydrol.2016.04.009.

Maraun, D., and Coauthors, 2010: Precipitation downscaling under climate change: Recent developments to bridge the gap between dynamical models and the end user. *Rev. Geophys.*, **48**, RG3003, doi:10.1029/2009RG000314.

Marhaento, H., M. J. Booij, and A. Y. Hoekstra, 2016: Attribution of changes in stream flow to land use change and climate change in a mesoscale tropical catchment in Java, Indonesia. *Hydrol. Res.*, **48**, 1143–1155, doi:10.2166/nh.2016.110.

Nicks, A. D., L. J. Lane, and G. A. Gander, 1995: Weather generator. USDA-Water Erosion Prediction Project: Hillslope Profile and Watershed Model Documentation, NSERL Rep.10, USDA-ARS, 2.1–2.22.

Nowreen, S., S. B. Murshed, A. K. M. S. Islam, B. Bhaskaran, and M. A. Hasan, 2015: Changes of rainfall extremes around the Haor basin area of Bangladesh using multi-member ensemble RCM. *Theor. Appl. Climatol.*, **119**, 363–377, doi:10.1007/s00704-014-1101-7.

Osca, J., R. Romero, and S. Alonso, 2013: Precipitation projections for Spain by means of a weather typing statistical method. *Global Planet. Change*, **109**, 46–63, doi:10.1016/j.gloplacha.2013.08.001.

Paredes, D., R. M. Trigo, R. Garcia-Herrera, and I. F. Trigo, 2006: Understanding precipitation changes in Iberia in early spring: Weather typing and storm-tracking approaches. *J. Hydrometeor.*, **7**, 101–113, doi:10.1175/JHM472.1.

Pavlik, D., D. Söhl, and T. Pluntke, 2014: Climate change in the Western Bug river basin and the impact on future hydroclimatic conditions. *Environ. Earth Sci.*, **72**, 4787–4799, doi:10.1007/s12665-014-3068-1.

Plummer, D. A., D. Caya, and A. Frigon, 2006: Climate and climate change over North America as simulated by the Canadian RCM. *J. Climate*, **19**, 3112–3132, doi:10.1175/JCLI3769.1.

Raje, D., and P. P. Mujumdar, 2011: A comparison of three methods for downscaling daily precipitation in the Punjab region. *Hydrol. Processes*, **25**, 3575–3589, doi:10.1002/hyp.8083.

Rockel, B., and K. Woth, 2007: Extremes of near-surface wind speed over Europe and their future changes as estimated from an ensemble of RCM simulations. *Climatic Change*, **81**, 267–280, doi:10.1007/s10584-006-9227-y.

Rudd, A.C., and A. L. Kay, 2016: Use of very high resolution climate model data for hydrological modelling: Estimation of potential evaporation. *Hydrol. Res.*, **47**, 660–670, doi:10.2166/nh.2015.028.

Rummukainen, M., 1997: Methods of statistical downscaling of GCM simulations. Rep. RMK 80, Swedish Meteorological and Hydrological Institute, 76 pp.

Sachindra, D. A., F. Huang, A. Barton, and B. J. C. Perera, 2013: Least square support vector and multi-linear regression for statistically downscaling general circulation model outputs to catchment streamflows. *Int. J. Climatol.*, **33**, 1087–1106, doi:10.1002/joc.3493.

Schoof, J. T., and S. C. Pryor, 2001: Downscaling temperature and precipitation: A comparison of regression-based methods and artificial neural networks. *Int. J. Climatol.*, **21**, 773–790, doi:10.1002/joc.655.

Schubert, S., and A. Henderson-Sellers, 1997: A statistical model to downscale local daily temperature extremes from synoptic-scale atmospheric circulation patterns in the Australian region. *Climate Dyn.*, **13**, 223–234, doi:10.1007/s003820050162.

Semenov, M. A., and E. M. Barrow, 1997: Use of a stochastic weather generator in the development of climate change scenarios. *Climatic Change*, **35**, 397–414, doi:10.1023/A:1005342632279.

Srinivas, V. V., B. Basu, D. N. Kumar, and S. K. Jain, 2014: Multisite downscaling of maximum and minimum daily temperature using support vector machine. *Int. J. Climatol.*, **34**, 1538–1560, doi:10.1002/joc.3782.

Suykens, J. A. K., and J. Vandewalle, 1999: Least squares support vector machine classifiers. *Neural Process. Lett.*, **9**, 293–300, doi:10.1023/A:1018628609742.

——, T. Van Gestel, J. De Brabanter, B. De Moor, and J. Vandewalle, 2002: *Least Squares Support Vector Machines*. World Scientific, 308 pp.

Tatsumi, K., T. Oizumi, and Y. Yamashiki, 2014: Assessment of future precipitation indices in the Shikoku region using a statistical downscaling model. *Stoch. Environ. Res. Risk Assess.*, **28**, 1447–1464, doi:10.1007/s00477-014-0847-x.

Taylor, K. E., R. J. Stouffer, and G. A. Meehl, 2012: An overview of CMIP5 and the experiment design. *Bull. Amer. Meteor. Soc.*, **93**, 485–498, doi:10.1175/BAMS-D-11-00094.1.

Tripathi, S., V. V. Srinivas, and R. S. Nanjundiah, 2006: Downscaling of precipitation for climate change scenarios: A support vector machine approach. *J. Hydrol.*, **330**, 621–640, doi:10.1016/j.jhydrol.2006.04.030.

van Vuuren, D. P., and Coauthors, 2011: The representative concentration pathways: An overview. *Climatic Change*, **109**, 5–31, doi:10.1007/s10584-011-0148-z.

Vapnik, V. N., 1998: *Statistical Learning Theory.* Wiley, 768 pp.

Wang, H., and D. Hu, 2005: Comparison of SVM and LS-SVM for regression. *Int. Conf. on Neural Networks and Brain*, Beijing, China, IEEE, 279–283, doi:10.1109/ICNNB.2005.1614615.

Wetterhall, F., S. Halldin, and C.-Y. Xu, 2005: Statistical precipitation downscaling in central Sweden with the analogue method. *J. Hydrol.*, **306**, 174–190, doi:10.1016/j.jhydrol.2004.09.008.

Wilby, R. L., and T. M. L. Wigley, 1997: Downscaling general circulation model output: A review of methods and limitations. *Prog. Phys. Geogr.*, **21**, 530–548, doi:10.1177/030913339702100403.

——, and C. W. Dawson, 2013: The statistical downscaling model: Insights from one decade of application. *Int. J. Climatol.*, **33**, 1707–1719, doi:10.1002/joc.3544.

——, T. M. L. Wigley, and D. Conway, 1998: Statistical downscaling of general circulation model output: A comparison of methods. *Water Resour. Res.*, **34**, 2995–3008, doi:10.1029/98WR02577.

——, D. Conway, and P. D. Jones, 2002a: Prospects for downscaling seasonal precipitation variability using conditioned weather generator parameters. *Hydrol. Processes*, **16**, 1215–1234, doi:10.1002/hyp.1058.

——, C. W. Dawson, and E. M. Barrow, 2002b: SDSM-a decision support tool for the assessment of regional climate change impacts. *Environ. Modell. Software*, **17**, 145–157, doi:10.1016/S1364-8152(01)00060-3.

Wilks, D. S., 1999a: Multisite downscaling of daily precipitation with a stochastic weather generator. *Climate Res.*, **11**, 125–136, doi:10.3354/cr011125.

——, 1999b: Simultaneous stochastic simulation of daily precipitation, temperature and solar radiation at multiple sites in complex terrain. *Agric. For. Meteor.*, **96**, 85–101, doi:10.1016/S0168-1923(99)00037-4.

Xu, C.-Y., 1999: From GCMs to river flow: A review of downscaling methods and hydrologic modelling approaches. *Prog. Phys. Geogr.*, **23**, 229–249, doi:10.1177/030913339902300204.

——, E. Widén, and S. Halldin, 2005: Modelling hydrological consequences of climate change—Progress and challenges. *Adv. Atmos. Sci.*, **22**, 789–797, doi:10.1007/BF02918679.

Xu, H., C.-Y. Xu, H. Chen, Z. Zhang, and L. Li, 2013: Assessing the influence of rain gauge density and distribution on hydrological model performance in a humid region of China. *J. Hydrol.*, **505**, 1–12, doi:10.1016/j.jhydrol.2013.09.004.

Zhang, X. C., 2005: Spatial downscaling of global climate model output for site-specific assessment of crop production and soil erosion. *Agric. For. Meteor.*, **135**, 215–229, doi:10.1016/j.agrformet.2005.11.016.

Zorita, E., and H. Von Storch, 1999: The analog method as a simple statistical downscaling technique: Comparison with more complicated methods. *J. Climate*, **12**, 2474–2489, doi:10.1175/1520-0442(1999)012<2474:TAMAAS>2.0.CO;2.